Sovereign Debt Pricing with Shifting Long-Run Growth Expectations

Sovereign Debt Pricing with Shifting Long-Run Growth Expectations

Pei Kuang*
University of Macau

Liang Shi†
University of Essex

March 2026

Abstract

The paper presents new evidence of systematic patterns in real-time estimates of long-run output growth rates and, importantly, reveals a negative, nonlinear relationship between these estimates and sovereign debt spreads during the Eurozone debt crisis of the 2010s. To study the implications of these beliefs, we develop a sovereign default model in which agents infer trend growth from aggregate output and from noisy signals about the trend. The model reproduces these empirical patterns in the trend growth estimates and their negative and nonlinear relationship with spreads, unlike a comparable full-information model. Overoptimism about trend growth during booms encourages excessive borrowing, leading to persistently elevated spreads thereafter.

Keywords: Long-run growth expectation, learning, long-term debts, European debt crises

JEL Codes: D83, H63, F41

*Department of Economics, University of Macau, E21B Avenida da Universidade, Taipa, Macau. E-mail: peikuang@um.edu.mo

†Institute for Social and Economic Research (ISER), University of Essex, Wivenhoe Park, CO4 3SQ, Colchester, United Kingdom. E-mail: shiliang369econ@gmail.com

1 Introduction

The sovereign debt crisis in the Eurozone during the 2010s has sparked significant interest in understanding the forces behind sovereign risk dynamics. While deteriorating fundamentals, such as slowing economic growth and rising public debt, are well-documented contributors, these alone do not fully explain the volatility in sovereign spreads (De Grauwe and Ji, 2013; Aizenman et al., 2013). A growing literature highlights the role of non-fundamental factors, including news shocks (Durdu et al., 2013; Dvorkin et al., 2020) and self-fulfilling equilibria (Bocola and Dovis, 2019; Ayres et al., 2025), suggesting that belief dynamics can shape sovereign debt spreads.

This paper focuses on the role of long-run output growth expectations in crisis-stricken GIIPS countries.[1] Intuitively, long-run growth and expectations about it directly affect the sustainability of sovereign debt, and hence influence sovereign spreads. We present two new strands of empirical evidence. **Evidence 1** documents systematic patterns in real-time estimates of potential GDP growth rates, and **Evidence 2** reveals a negative, nonlinear relationship between real-time potential output growth estimates and sovereign debt spreads, whereby spreads become more sensitive to economic shocks when those estimates are low. These observations raise a natural question: To what extent do shifting long-run growth expectations influence sovereign debt dynamics?

To answer this question, we develop a canonical sovereign default model in the tradition of Eaton and Gersovitz (1981), Aguiar and Gopinath (2006), and Chatterjee and Eyigungor (2012). The sovereign receives an exogenous stochastic output income with both cyclical and trend components and issues long-maturity defaultable bonds. Risk-neutral foreign creditors price these bonds by accounting for default risk. Motivated by Evidence 1, we deviate from the standard full-information rational expectations (RE) model by assuming agents cannot observe the true trend and cycle components of GDP growth, but instead infer them from observed output and a noisy signal for the trend (Boz et al., 2011).

The model successfully matches Evidence 1 even though cyclical fluctuations dominate output dynamics.[2] Given the noisiness of trend signals, agents place substantial weight on

[1] GIIPS refers to Greece, Ireland, Italy, Portugal, and Spain.

[2] See Boz et al. (2011) and Garcia-Cicco et al. (2010) for evidence on the dominance of cyclical components in exogenous productivity.

recent output realizations when updating beliefs about trend growth. Consequently, negative (positive) cyclical shocks tend to induce pessimism (optimism) about the trend, generating persistent errors in beliefs and a positive correlation between estimates of trend growth and cycle. As cyclical shocks are frequently misinterpreted as changes in trend, boom–bust cycles – the typical drivers of sovereign default episodes – systematically generate overestimation of trend growth during booms and underestimation during crises.

The learning mechanism helps generate the spread dynamics highlighted in Evidence 2. A comparable full-information RE model generates little correlation between spreads and trend growth, since trend and cycle are independent and cyclical shocks dominate output dynamics. By contrast, in the learning model, the comovement of trend and cycle beliefs leads to more frequent optimism-pessimism shifts in expected long-term repayment capacity, thereby strengthening the negative correlation between trend growth estimates and spreads.

Sovereign default risk further amplifies these dynamics, giving rise to the nonlinear response of spreads around crises. During booms, optimism about the trend growth lowers spreads and encourages greater borrowing. Combined with the mean-reverting of the output growth, such over borrowing causes spreads to rise subsequently. In recessions, pessimism about the trend growth worsens repayment prospects, raising spreads even further. When debt ratios are already high, repeated negative shocks steepen the yield curve, and the sovereign may cut issuance – but typically not enough to offset the upward pressure on spreads. By contrast, under full information there is no trend misperception, so debt over-accumulation in booms and pessimism-driven spread surges in downturns do not arise. This leads to fewer defaults, lower average spreads, and higher sustainable debt ratios. These findings highlight the importance of improving the accuracy of real-time trend growth estimates.

The remainder of the paper is structured as follows: Section 1.1 discusses related literature. Section 2 presents new empirical evidence. Section 3 outlines the setup of a sovereign default model with learning about the long-run output growth rates. Section 4 details the calibration strategy and demonstrates the model's fit to Portuguese data. Section 5 discusses the quantitative results, including the model's replication of empirical evidence and the mechanism, and the consequences of overestimated trend growth during booms on future debt dynamics. Section 6 concludes.

1.1 Related literature

This paper is closely related to the literature on quantitative sovereign default models. Our full-information model builds on the framework of Aguiar and Gopinath (2006), who highlight the importance of stochastic trend shocks in understanding default frequency. Since then, advancements of this literature include analyzing the role of long-maturity debt in generating high spreads and default frequency (Chatterjee and Eyigungor, 2012) and the inclusion of debt renegotiation (Yue, 2010; Mihalache, 2020), and further analysis of the role of trend and cyclical endowments in the default model (Aguiar et al., 2016). Literature concerning the 2010s EU debt crisis includes Arellano and Bai (2017) and Na et al. (2018), among others. This paper contributes to the literature by documenting persistent real-time misperceptions of long-run growth and by showing, within a quantitative sovereign default framework, that such misperceptions can generate nonlinear sovereign spread dynamics.

Although sovereign debt spreads are strongly linked to fundamentals, empirical evidence shows that this link is not complete: sizable defaults have occurred during favorable times (Tomz and Wright, 2007), and spreads can also be driven by investor sentiment (De Grauwe and Ji, 2013). An extensive literature has explored non-fundamental drivers in the quantitative sovereign default framework. Durdu et al. (2013) and Dvorkin et al. (2020) relax the full-information assumption by incorporating news shocks about productivity, which influence expectations about next-period productivity and hence agents' debt issuance choices and pricing. Recently, Paluszynski (2023) documents significant output growth forecast errors around the time of the Global Financial Crisis. He calibrates a model with learning about the realization of rare disaster shocks that negatively affect income to Portugal. The model rationalizes the delayed increase in bond spreads relative to the rise in debt-to-GDP ratios. Niemann and Prein (2025) find evidence of diagnostic expectations in IMF growth forecasts and incorporate overreaction to news into a canonical sovereign default model. Their framework matches key business cycle statistics and is used to evaluate the implications of fiscal rules. We contribute to this literature by exploring the relevance of imperfect knowledge and learning about long-run growth.

A related literature analyzes non-fundamental forces in the sovereign default framework based on self-fulfilling debt crises and multiple equilibria. Lorenzoni and Werning (2019) provide a detailed analysis of how initial debt levels, fiscal policy regimes, and debt maturity

structures influence a country's vulnerability to crises. Focusing on shifts in the maturity structure, Bocola and Dovis (2019) find that self-fulfilling default played a limited role in Italy's debt crisis. Ayres et al. (2025) demonstrate that expectations of high-spread equilibria can significantly raise spreads during persistent stagnation. Theoretical investigations of the mechanisms behind multiple equilibria in sovereign default models include Auclert and Rognlie (2016), Stangebye (2020), and Aguiar and Amador (2020). Our results complement this literature by highlighting an alternative mechanism based on persistent misperceptions of long-run growth.

Our paper is also related to the wider literature on imperfect information in macroeconomics, including Eusepi and Preston (2011), Schmitt-Grohé and Uribe (2012), Adam et al. (2012), Kuang (2014) and Kuang et al. (2026). Regarding long-run growth perceptions, Boz et al. (2011) assume that agents cannot distinguish between cyclical and trend growth rates. Kuang and Mitra (2016) emphasize the critical role of learning about trend growth in understanding business cycles. Growth forecast errors have also been linked to the unintended effects of fiscal policy. For example, Blanchard and Leigh (2013, 2014) show that fiscal consolidations during the early Great Financial Crisis were often followed by lower-than-expected growth. Kuang and Mitra (2025) document systematic forecast errors in Eurozone long-run growth projections and their role in prolonged austerity, which stems from fiscal rules built on structural balance estimation. Kuang et al. (2024) analyze the welfare properties of different statistical filtering and structural methods in estimating output gaps in real time in New Keynesian models. By contrast, this paper studies how imperfect information and learning about long-run growth shape sovereign debt issuance and crisis dynamics, complementing work such as Cole et al. (2025) that emphasizes information frictions in sovereign debt markets during the Eurozone crisis.

2 Empirical evidence

Long-run output growth is a key determinant of repayment capacity for countries issuing defaultable sovereign debt, and international creditors rely on real-time estimates to adjust evaluations of long-term repayment prospects and debt prices. This section presents new evidence on systematic patterns in these estimates for 11 Eurozone countries. We use annual data

from 1999 to 2019, covering the Eurozone sovereign debt crisis of the 2010s. The countries include GIIPS countries (Greece, Ireland, Italy, Portugal, Spain) that were subject to substantial sovereign default risks and non-GIIPS economies (Austria, Belgium, Finland, France, Germany, Netherlands) that were considered safe for comparison purposes.

Real-time trend growth estimates are taken from the European Commission's European Economic Forecast (EEF) and the IMF's World Economic Outlook (WEO), published in the spring of the year following the one being estimated.[3] We use the real-time estimates of the potential output growth rate as our measure of the "trend growth estimate" (denoted $\tilde{\gamma}_t$), and the real-time output gap estimate as our measure of the "cycle estimate" (denoted $\tilde{z}_t$). Specifically, for each calendar year t, the EEF and WEO publish estimates of potential output growth and output gap in the following spring (typically in April), i.e., in year $t+1$. We treat these spring publications as the real-time estimates for year t.[4]

2.1 Systematic errors in real-time potential GDP growth estimates

We document new evidence on systematic errors in real-time potential GDP growth estimates: (i) a positive and large autocorrelation in estimation errors, (ii) a strong positive correlation between real-time estimates of potential output growth and the output gap, and (iii) systematic overestimation prior to the 2010s debt crisis and underestimation during it. We start by analyzing the persistence of errors, measured by $\tilde{\gamma}_t^{i,err} = \tilde{\gamma}_t^i - \gamma_t^i$, where i denotes country, t covers annual observations for 1999–2019, and γ_t^i denotes an *ex post* statistical trend estimate constructed using a broader 1995–2022 sample.[5] Using the HP filter (Hodrick and Prescott, 1997) to obtain γ_t^i, we estimate the autocorrelation coefficient for these errors, i.e., $\hat{\rho}(\tilde{\gamma}_t^{i,err})$.

[3] We do not use datasets on professional forecasts, such as Consensus Economics, as they typically do not contain real-time estimates of the output gap and potential output, which are central to our analysis. Moreover, Paluszynski (2023) shows that forecast errors for one-year-ahead real GDP from Consensus Economics are quantitatively similar to those from the OECD, IMF, and European Commission. It is widely documented that forecast errors from private-sector sources are comparable to those from international institutions such as the European Commission, OECD, and IMF (Chabin et al., 2020; Celasun et al., 2021).

[4] In the spring of year t, the EEF typically provides forecasts of potential GDP growth and output gaps for years t and $t+1$, along with estimates for several previous years. The IMF provides forecasts of output and output gaps for years t and $t+1$, and retrospective estimates for a longer history (extending to 1980). We calculate WEO's real-time estimate of potential output growth by utilizing its real-time estimates of output gap and actual GDP.

[5] Online Appendix A reports descriptive statistics for $\tilde{\gamma}_t^{i,err}$ (mean, standard deviation, and root mean squared error) and its components for the full sample and for sub-samples. Note that these "estimation errors" do not refer to deviations of real-time estimates from a latent true trend or from full-information beliefs.

As reported in columns 1 and 3 of Table 1, estimated autocorrelation coefficients are generally positive, large and statistically significant at conventional significance levels. These coefficients are particularly high among GIIPS countries. Moreover, we observe strong positive correlations between real-time estimates of potential output growth $\tilde{\gamma}_t^i$ and the output gap $\tilde{z}_t^i$ among GIIPS countries (columns 2 and 4), whereas the HP-filtered trend growth γ_t^i and cycle z_t^i show little to no correlation (column 5).

Table 1: Systematic errors in real-time potential GDP growth estimates ($\tilde{\gamma}_t^i$)

	EEF data		WEO data		
	$\hat{\rho}(\tilde{\gamma}_t^{i,err})$	$corr(\tilde{\gamma}_t^i, \tilde{z}_t^i)$	$\hat{\rho}(\tilde{\gamma}_t^{i,err})$	$corr(\tilde{\gamma}_t^i, \tilde{z}_t^i)$	$corr(\gamma_t^i, z_t^i)$
Greece	0.90***	0.97***	0.67***	0.79***	0.15
Ireland	0.83***	0.69***	0.74**	0.63***	0.14
Italy	0.67***	0.63***	−0.01	0.36	0.26
Portugal	0.72***	0.61***	0.79***	0.53**	0.43**
Spain	0.78***	0.68***	0.82**	0.74***	0.13
Austria	0.67***	0.26	0.50**	-0.01	0.03
Belgium	0.58***	0.30	0.42**	0.29	0.12
Finland	0.66***	0.56***	0.47**	0.61***	0.27
France	0.59***	0.34	0.68***	0.68**	0.17
Germany	0.23	0.15	0.33	0.23	0.03
Netherlands	0.60**	0.39	0.39	0.65***	0.45**

Notes: $\hat{\rho}(\tilde{\gamma}_t^{i,err})$ refers to the estimated autoregressive coefficient $\hat{\rho}$ in the regression $\tilde{\gamma}_t^{i,err} = \rho\tilde{\gamma}_{t-1}^{i,err} + u_t^i$, where $\tilde{\gamma}_t^{i,err} \equiv \tilde{\gamma}_t^i - \gamma_t^i$ and γ_t^i is the HP-filtered trend growth (smoothing parameter = 100). In the last column, $corr(\gamma_t^i, z_t^i)$ denotes the correlation between HP-filtered GDP trend growth and cycles. In the WEO database, potential growth and output gap estimates for Greece are unavailable for 2003–2008. Descriptive statistics for $\tilde{\gamma}_t^{i,err}$ are reported in Table A.1 of the Online Appendix. *** denotes p-value below 0.01, ** denotes p-value below 0.05.

We interpret these findings as evidence of persistent real-time belief dynamics in trend growth estimates, rather than as deviations from a real-time full-information benchmark. Taking the ex post HP-filtered trend growth as a benchmark, the high autocorrelation in $\tilde{\gamma}_t^{i,err}$ indicates that real-time estimation errors are not white noise.[6] The strong correlation between $\tilde{\gamma}_t^i$ and $\tilde{z}_t^i$ further suggests that long-run growth estimation is likely influenced by

[6]As discussed by Edge et al. (2007) and Kuang and Mitra (2016), HP-filtered trend growth is often treated as an ex post estimate of long-run growth that incorporates information unavailable in real time. We use this object as a retrospective statistical benchmark, not as the trend that would be observed by fully informed agents at time t. Real-time estimates published by policymaking institutions are typically produced using a production function approach or statistical filtering methods, based solely on information available up to time t (see, for example, Havik et al. (2014)). These two approaches generally yield similar estimates of potential output (see the discussion in Appendix D of the Irish Fiscal Advisory Council (2013)).

cyclical conditions. Consistent with this finding, Coibion et al. (2018) show that potential output estimates produced by policymaking institutions are highly responsive to transitory economic shocks.

To test robustness, we replicate Table 1 using alternative standard macroeconomic filters: the Christiano-Fitzgerald (CF) filter (Christiano and Fitzgerald, 2003), the Baxter-King (BK) filter (Baxter and King, 1999), and the Hamilton filter (Hamilton, 2018). As reported in Table B.1 in the Online Appendix, the CF and BK filters yield broadly similar patterns to the HP filter.[7]

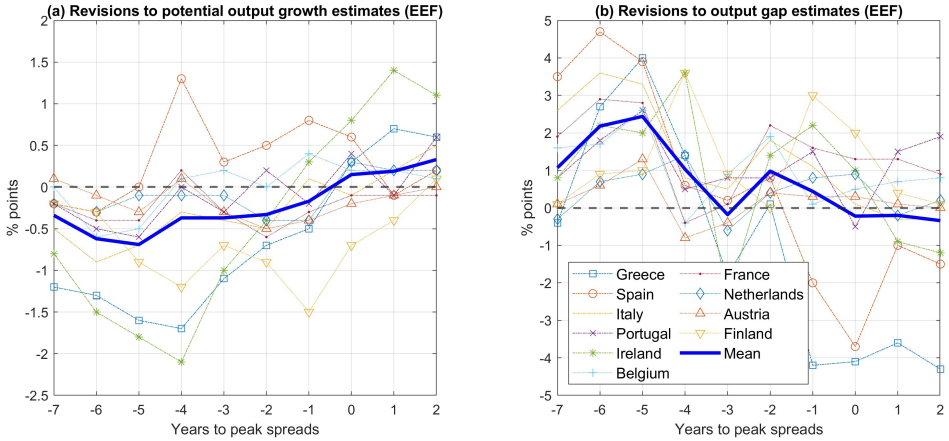

Figure 1: Revisions of potential growth and output gap estimates: ex post estimates made in 2020 Q3 minus real-time estimates. The horizontal axis shows years relative to the peak years of sovereign debt spreads: 2011 for Ireland and Finland, 2012 for other countries. For example, -1 on the horizontal axis indicates year 2010 for Ireland and Finland, and 2011 for other countries. Data are from EEF, covering estimates for years 2004 - 2014. We confirm that excluding non-GIIPS countries yields similar mean revisions.

Figure 1 illustrates systematic revisions to real-time potential GDP growth rates for EU countries, based on two vintages of estimates. Revisions are calculated as 2020 Q2 estimates minus real-time estimates. The negative revisions to potential output growth when $h \leq -1$ in panel (a) suggest that real-time estimates were systematically overoptimistic before and during the early phase of the Eurozone debt crisis. After $h = -1$, $\tilde{\gamma}_t^i$ revisions turn positive, implying that real-time estimates were more pessimistic than ex post estimates.[8] Meanwhile,

[7]By contrast, the Hamilton filter delivers insignificant $\hat{\rho}(\tilde{\gamma}_t^{i,err})$ and mostly insignificant $corr(\gamma_t^i, z_t^i)$. This reflects its one-sided design: Hamilton constructs the trend as the forecastable component of future output using only past values, so deviations from real-time estimates tend to exhibit weaker persistence. In contrast, the HP, CF, and BK filters are two-sided smoothers that use both past and future data to extract low-frequency components, resulting in smoother retrospective trend series. These results suggest that the persistence documented using two-sided filters is not mechanically implied by real-time filtering alone.

[8]Online Appendix B shows that the results are robust to using WEO potential output estimates instead of EEF estimates, and to using ex post HP-filtered trend growth rates instead of those produced by the European

revisions to output gaps in panel (b) are generally positive (underestimation of z_t^i in real time) before $h = -1$, but negative thereafter (real-time overestimation of z_t^i).[9] We now summarize the above findings as follows.

Evidence 1 (Systematic patterns in real-time potential GDP growth estimates):

(i) Real-time estimation errors of potential output growth tend to exhibit strong positive autocorrelation (see columns 1 and 3 in Table 1).

(ii) Real-time potential output growth estimates are strongly positively correlated with real-time output gap estimates (see columns 2 and 4 in Table 1).

(iii) Revisions to potential output growth estimates indicate over-optimism before the debt crisis and over-pessimism during it (see Figure 1).

In the model section, we replicate Evidence 1(i) and (ii) by calibrating a learning mechanism in which agents partially confuse trend output growth with the cycle and hence generate persistent belief errors about trend growth and a positive correlation between estimates of trend growth and cycle. Importantly, in mapping Evidence 1(i)–(ii) to the model, we do not interpret the ex post filtered trend as a real-time full-information object; rather, we assess whether learning can reproduce the observed persistence and comovement in real-time estimates. Because boom–bust fluctuations in the cycle are the typical drivers of sovereign default episodes in the canonical sovereign default framework, this tight comovement between trend and cycle beliefs generates overestimated trend growth during booms (before crises) and underestimated trend growth during busts (crises), in line with Evidence 1(iii).

2.2 A negative and nonlinear relationship between real-time potential GDP growth estimates and sovereign debt spreads

Given the critical role for beliefs about potential GDP growth rates in determining sovereign debt spreads and that these estimates exhibit systematic errors, an important question is how

Commission.

[9] We also regress estimation errors in trend growth estimates on revisions to output gap estimates at the individual country level, in the spirit of Coibion and Gorodnichenko (2015) and Adam et al. (2025). This is a test of RE. We find that the regression coefficients are generally insignificant from zero (see Online Appendix B for further details), implying that RE given real-time information is not rejected, consistent with the assumption of imperfect information RE in the paper.

these estimates relate to sovereign debt spreads, particularly during the 2010s European debt crisis. We find that the relationship is significant, negative, and nonlinear.

Table 2: Correlation between sovereign bond spreads and real-time trend growth estimates $corr(rs_t^i, \tilde{\gamma}_t^i)$, and the correlation between spreads and filtered trend growth rates $corr(rs_t^i, \gamma_t^i)$

	$corr(\tilde{\gamma}_t^i, rs_t^i)$		$corr(\gamma_t^i, rs_t^i)$			
	EEF data	WEO data	HP	CF	BK	Hamilton
Greece	-0.83^{***}	-0.72^{***}	-0.05	-0.08	-0.07	-0.37
Ireland	-0.79^{***}	-0.69^{***}	0.18	0.02	0.01	-0.40
Italy	-0.79^{***}	-0.71^{***}	-0.74^{***}	-0.58^{***}	-0.66^{***}	-0.43
Portugal	-0.71^{***}	-0.73^{***}	-0.58^{***}	-0.45^{**}	-0.58	-0.53^{**}
Spain	-0.85^{***}	-0.88^{***}	-0.73^{***}	-0.82^{***}	-0.82^{***}	-0.84^{***}
Austria	-0.60^{***}	-0.41	-0.55^{***}	-0.61^{***}	-0.66^{***}	-0.17
Belgium	-0.56^{**}	-0.73^{***}	-0.54^{**}	-0.56^{***}	-0.64^{***}	-0.40
Finland	-0.58^{**}	-0.59^{**}	-0.37	-0.38	-0.39	-0.04
France	-0.77^{***}	-0.89^{***}	-0.76^{***}	-0.76^{***}	-0.80^{***}	-0.66^{***}
Netherlands	-0.65^{***}	-0.77^{***}	-0.65^{***}	-0.67^{***}	-0.72^{***}	-0.31

Notes: Spreads are retrieved from St. Louis Fed. GDP data used for filtering are taken from Eurostat, 1995-2022. The HP-filtered trends reported on the right panel use a smoothing parameter of 100. For the Hamilton filter, we set lead = 2 and a lag = 1. For CF and BK filters, the parameter for the lower cutoff is 2, the upper cutoff is 8, and the lag length is 3, all suitable for annual frequency. All filtering calculations are implemented using MATLAB's built-in functions from the Econometrics Toolbox. *** denotes p-value below 0.01, ** denotes p-value below 0.05.

Columns 1–2 of Table 2 report strong negative correlations between 10-year government bonds over the German counterpart (rs_t^i) and real-time potential output growth estimates ($\tilde{\gamma}_t^i$) for GIIPS countries. For example, the absolute values of correlation coefficients are above 0.71 for EEF data and above 0.69 for WEO data. Among non-GIIPS countries, the correlations are generally somewhat weaker but remain statistically significant. By contrast, the filtered trend growth (γ_t^i) exhibits weaker and frequently insignificant correlations with spreads. The weaker relationship with filtered trend growth may reflect that markets overreact to short-term fluctuations. Moreover, imperfect perceptions of long-run growth are likely priced in sovereign bond spreads.

Figure 2 illustrates a nonlinear relationship between real-time potential GDP growth estimates and spreads in GIIPS countries. As shown in panels (a) and (b), the negative relationship is especially steep once $\tilde{\gamma}_t^i$ falls below the zero-growth threshold, or during the 2008–2015

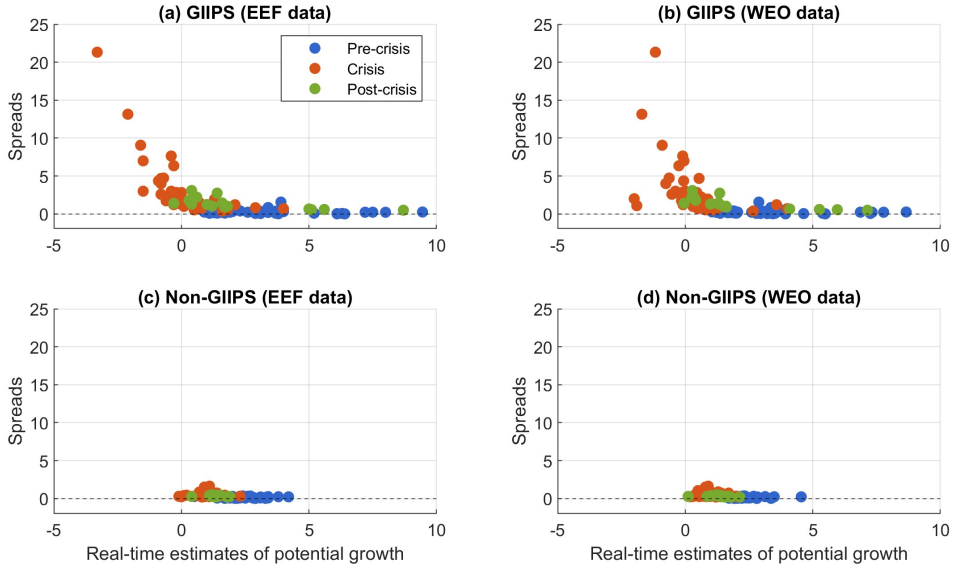

Figure 2: A negative and non-linear (linear) relationship between sovereign bond spreads rs_t^i and real-time trend growth estimates $\tilde{\gamma}_t$ for GIIPS countries (non-GIIPS countries), both in percentage points. The figure uses annual Data between 1999 and 2019. Greek data after default (2013-2019) are excluded. "Pre-crisis" period refers to year 1999-2007, "Crisis" to 2008–2015, and "Post-crisis" to 2016–2019. Left (Right) panels correspond to EEF (WEO) database. Non-GIIPS countries are Austria, Belgium, Finland, France and Netherlands, as German government bond spreads are used as the risk-free rate. Figure C.1 of the Online Appendix excludes outliers in GIIPS data, and the nonlinearity still exists.

crisis period (red points). For non-GIIPS countries (panels (c) and (d)), the relationship appears much weaker, with spreads generally remaining below 2%.

To formally test the nonlinearity, we estimate the following panel regression model:

$$rs_t^i = \theta_i + \xi_t + \beta_{\tilde{\gamma},l} I_t^{l,i} \tilde{\gamma}_t^i + \beta_{\tilde{\gamma},m} I_t^{m,i} \tilde{\gamma}_t^i + \beta_{\tilde{\gamma},h} I_t^{h,i} \tilde{\gamma}_t^i + \beta_b \Delta(b_t^i/y_t^i) + \beta_{\tilde{z}} \tilde{z}_t^i + u_t^i, \tag{1}$$

where rs_t^i is the spread in basis points (bps), $I_t^{l,i}$, $I_t^{m,i}$, and $I_t^{h,i}$ are binary variables for low, medium, and high regimes of the real-time trend growth estimate $\tilde{\gamma}_t^i$, defined using the 25th and 75th percentiles of its empirical distribution.[10] θ_i and ξ_t denote country and year fixed effects. We include two controls: (i) the first difference of the debt-to-GDP ratio $\Delta(b_t^i/y_t^i)$, and (ii) the real-time output gap estimate $\tilde{z}_t^i$. For comparison, we also estimate a simpler linear model:

$$rs_t^i = \bar{\theta}_i + \bar{\xi}_t + \bar{\beta}_{\tilde{\gamma}} \tilde{\gamma}_t^i + \bar{\beta}_b \Delta(b_t^i/y_t^i) + \bar{\beta}_{\tilde{z}} \tilde{z}_t^i + \bar{u}_t^i. \tag{2}$$

[10]We choose these percentiles to balance extremeness with the number of observations in the sub-samples. We report regime-specific values of real-time potential growth estimates, sample sizes, and country-year coverage in Online Appendix Table C.2.

We estimate both the nonlinear and linear specifications for the full sample of 10 EU countries, GIIPS countries only, and non-GIIPS countries only.[11]

Table 3: The nonlinear relationship between spreads and real-time trend growth estimates

	EEF data			WEO data		
	All	GIIPS	Non-GIIPS	All	GIIPS	Non-GIIPS
Linear regression (2)						
$\tilde{\gamma}_t^i$	-65.9^{***}	-65.1^{***}	-15.5^{***}	-69.4^{***}	-72.8^{***}	-19.5^{***}
	(10.2)	(15.4)	(3.7)	(12.1)	(19.5)	(3.8)
Control: $\tilde{z}_t^i$	-33.0^{***}	-48.5^{***}	0.46	-26.6^{***}	-43.9^{***}	1.9
	(6.5)	(10.5)	(1.82)	(7.6)	(13.3)	(1.9)
Control: $\Delta(b_t^i/y_t^i)$	-4.5^{**}	-6.0^{**}	1.7^{**}	-3.3	-4.1	1.5^{**}
	(2.0)	(3.0)	(0.75)	(3.4)	(19.5)	(0.7)
R^2	0.51	0.59	0.31	0.37	0.45	0.36
Nonlinear regression (1)						
Low $\tilde{\gamma}_t^i$	-343.1^{***}	-470.6^{***}	14.2	-192.8^{***}	-181.3^{***}	7.9
	(23.7)	(37.9)	(9.4)	(36.2)	(67.7)	(13.2)
Medium $\tilde{\gamma}_t^i$	-80.4^{***}	-40.0^{***}	-9.3	-95.0^{***}	-92.4^{**}	-14.1^{**}
	(14.6)	(19.5)	(5.4)	(19.4)	(36.4)	(6.3)
High $\tilde{\gamma}_t^i$	-44.8^{***}	-22.3^{**}	-10.5^{***}	-61.7^{***}	-57.6^{***}	-14.6^{***}
	(7.6)	(10.5)	(3.7)	(11.7)	(20.5)	(4.3)
R^2	0.74	0.84	0.41	0.43	0.48	0.40
Observations	183	88	95	177	82	95

Notes: Panel regression estimates from equations (1) and (2), testing for nonlinear effects of real-time potential growth estimates ($\tilde{\gamma}_t^i$ in percentage points) on sovereign bond spreads (rs_t^i in basis points). Details of controls for "Nonlinear regression" are reported in Table C.1, Online Appendix. Sample: 2001–2019 (limited by debt data availability), with Greece post default (after 2012) excluded; WEO omits Greece 2003–2008. Non-GIIPS: Austria, Belgium, Finland, France, Netherlands. Standard errors in parentheses. *** denotes p-value below 0.01, ** denotes p-value below 0.05.

Table 3 summarizes estimation results for regressions (1) and (2). For GIIPS countries, a one-percentage-point reduction in EEF estimates of $\tilde{\gamma}_t^i$ is associated with a 65 bps increase in spreads in the linear model. According to the nonlinear model, under low $\tilde{\gamma}_t^i$ regimes, the effect intensifies dramatically to 471 bps. Under medium and high regimes, the negative coefficients are smaller but still vary by regime. These findings confirm the nonlinear relationship between $\tilde{\gamma}_t^i$ and rs_t^i among GIIPS countries, as well as in the full sample (columns labeled "All"). By

[11]Table C.3 (Online Appendix C.1) reports a "horse race" regression illustrating the incremental predictive power of real-time trend growth estimates for sovereign spreads relative to conventional control variables.

contrast, non-GIIPS countries exhibit much smaller and often insignificant effects under low $\tilde{\gamma}_t^i$ regimes, possibly reflecting better growth expectations and greater financial resilience during the crisis. We summarize the above results as follows.

Evidence 2 (A negative and nonlinear relationship between real-time potential GDP growth estimates and sovereign debt spreads):

(i) Sovereign bond spreads for the 10 eurozone countries are strongly negatively correlated with real-time potential output growth estimates (see columns 1 and 2 of Table 2). By contrast, filtered trend growth measures are less correlated with spreads (see columns 3 - 6 of Table 2).

(ii) The relationship between sovereign bond spreads and real-time potential output growth estimates for GIIPs countries is negative and nonlinear: when trend-growth estimates are already low, a change in potential output growth estimates (e.g., a decline) is associated with a disproportionately larger change (e.g. increase) in sovereign bond spreads (see panel a and b of Figure 2 and columns 2 and 5 of Table 3).

In our model, subjective estimates of trend growth comove with those of the cycle, which is the primary driver of spread dynamics, contributing to replicate Evidence 2(i). The state-dependent sensitivity of spreads to trend beliefs contributes to both Evidence 2(i) and (ii): when debt-to-GDP ratios are low, lower trend growth can slightly reduce spreads by prompting deleveraging, whereas under high ratios, lower trend growth substantially raises spreads by heightening default risk.

3 The model

How does imperfect knowledge about long-run growth affect sovereign debt markets and the broader economy? To address this question, we embed a learning mechanism for trend growth into a canonical sovereign default framework à la Eaton and Gersovitz (1981) and Chatterjee and Eyigungor (2012). We begin by describing the decomposition of output into trend and cyclical components (Section 3.1), then introduce the learning rule that agents in the imperfect information (II) model use to form beliefs (Section 3.2). Section 3.3 presents the II model,

where decisions are based on beliefs, and shows how the full-information (FI) model emerges as a special case, providing a natural benchmark for comparison.

3.1 The exogenous output process

We begin by specifying the true exogenous output process that drives the sovereign's economy. Output Y_t consists of a cyclical component z_t and a trend component γ_t, following the standard decomposition in Aguiar and Gopinath (2006):

$$Y_t = e^{z_t}\Gamma_t, \tag{3}$$

where z_t represents the cycle and Γ_t is the cumulative product of trend growth.[12]

$$z_t = \rho_z z_{t-1} + \varepsilon_t^z, \tag{4}$$

with $|\rho_z| < 1$ and ε_t^z is identically and independently normally distributed, i.e., $\varepsilon_t^z \sim i.i.N(0, \sigma_z^2)$. Γ_t represents the cumulative product of the trend:

$$\Gamma_t = e^{\gamma_t}\Gamma_{t-1} = \prod_{\tau=0}^{t} e^{\gamma_\tau}, \tag{5}$$

where the trend growth rate γ_t follows:

$$\gamma_t = (1-\rho_\gamma)\overline{\gamma} + \rho_\gamma \gamma_{t-1} + \varepsilon_t^\gamma, \tag{6}$$

with $|\rho_\gamma| < 1$ and $\varepsilon_t^\gamma \sim i.i.N(0, \sigma_\gamma^2)$, and $\overline{\gamma}$ denoting the long-run average output growth rate.

3.2 Learning about the trend

To reconcile the empirical evidence in the II model, we assume that both the true trend and cyclical components of the output process are unobservable, requiring agents to form beliefs about the growth rate of the trend output $\tilde{\gamma}_t$ and the cyclical output $\tilde{z}_t$ for decision-making.

[12] Based on the definition of the output process, the output gap relative to potential (or trend) output is given by $(Y_t - Y_t^p)/Y_t^p \equiv (e^{z_t}\Gamma_t - \Gamma_t)/\Gamma_t = e^{z_t} - 1$, which is consistent with the output gap measure used in the EEF and WEO databases.

We adopt the learning rule from Boz et al. (2011), which provides a tractable mechanism for this type of misperception. Belief formation is based on the structure of the output process and observed output growth:

$$\Delta \log(Y_t) \equiv \log\left(\frac{e^{z_t}\Gamma_t}{e^{z_{t-1}}\Gamma_{t-1}}\right) = z_t - z_{t-1} + \gamma_t, \tag{7}$$

and on a noisy signal s_t about trend growth:

$$s_t = \gamma_t + n_t, \qquad n_t = \rho_n n_{t-1} + \varepsilon_t^n, \tag{8}$$

where $\varepsilon_t^n \sim i.i.N(0, \sigma_n^2)$ is white noise capturing deviations of the signal from the true trend. Agents are assumed to know the structure of $\Delta \log(Y_t)$ and the stochastic process for n_t. The belief structure is summarized by the following state-space model. The *observation equation* relates observed output growth and the trend signal to the unobserved state vector $\boldsymbol{\alpha}_t$: $\mathbf{Y}_t = \mathbf{Z}\boldsymbol{\alpha}_t$, or equivalently:

$$\begin{bmatrix} \Delta \log(Y_t) \\ s_t \end{bmatrix} = \begin{bmatrix} 1 & -1 & 1 & 0 \\ 0 & 0 & 1 & 1 \end{bmatrix} \cdot \begin{bmatrix} z_t \\ z_{t-1} \\ \gamma_t \\ n_t \end{bmatrix}. \tag{9}$$

The *transition equation* describes the evolution of the unobserved variables $\boldsymbol{\alpha}_t = (z_t, z_{t-1}, \gamma_t, n_t)$ as: $\boldsymbol{\alpha}_t = \mathbf{T}\boldsymbol{\alpha}_{t-1} + \mathbf{C} + \mathbf{R}\boldsymbol{\eta}_t$, or equivalently:

$$\begin{bmatrix} z_t \\ z_{t-1} \\ \gamma_t \\ n_t \end{bmatrix} = \begin{bmatrix} \rho_z & 0 & 0 & 0 \\ 1 & 0 & 0 & 0 \\ 0 & 0 & \rho_\gamma & 0 \\ 0 & 0 & 0 & \rho_n \end{bmatrix} \begin{bmatrix} z_{t-1} \\ z_{t-2} \\ \gamma_{t-1} \\ n_{t-1} \end{bmatrix} + \begin{bmatrix} 0 \\ 0 \\ (1-\rho_\gamma)\overline{\gamma} \\ 0 \end{bmatrix} + \begin{bmatrix} 1 & 0 & 0 \\ 0 & 0 & 0 \\ 0 & 1 & 0 \\ 0 & 0 & 1 \end{bmatrix} \begin{bmatrix} \varepsilon_t^z \\ \varepsilon_t^\gamma \\ \varepsilon_t^n \end{bmatrix}. \tag{10}$$

Here, $\boldsymbol{\eta}_t \sim i.i.N(0, \boldsymbol{Q})$ and $\boldsymbol{Q} = \text{diag}(\sigma_z^2, \sigma_\gamma^2, \sigma_n^2)$. As $\sigma_n \to +\infty$, the signal becomes uninformative about the trend, leading agents to rely more heavily on observed output growth and thus on cyclical shocks z_t and z_{t-1}. Conversely, as $\sigma_n \to 0$, the signal becomes perfectly accurate, allowing agents to form trend beliefs independently of cyclical fluctuations.

Given the state-space model, agents form optimal estimates $\mathbf{a}_t$ of the unobserved variables

$\boldsymbol{\alpha}_t$ using Bayesian updating. The prior estimate is given by $\mathbf{a}_{t|t-1} = \mathbf{T}\mathbf{a}_{t-1} + \mathbf{C}$, while the posterior estimate $\mathbf{a}_t$ combines the prior with new observations:

$$\mathbf{a}_t = \kappa^1 \mathbf{a}_{t|t-1} + \kappa^2 \mathbf{Y}_t, \tag{11}$$

where the gain matrices are defined as $\kappa^1 = [\mathbf{I} - \mathbf{P}\mathbf{Z}'(\mathbf{Z}\mathbf{P}\mathbf{Z}')^{-1}\mathbf{Z}]$ and $\kappa^2 = \mathbf{P}\mathbf{Z}'(\mathbf{Z}\mathbf{P}\mathbf{Z}')^{-1}$.[13] Here, $\mathbf{I}$ denotes a 4×4 identity matrix. The vector $\mathbf{a}_t = [\tilde{z}_t, \tilde{z}_{t-1}, \tilde{\gamma}_t, \tilde{n}_t]^T$ represents agents' beliefs about the exogenous state vector. While this learning mechanism generates local deviations of beliefs from the true underlying stochastic trend and cycle, it does not induce permanent divergence.

3.3 The imperfection information (II) model

The sovereign maximizes expected discounted utility from consumption C_t:

$$\mathbb{E}_0 \sum_{t=0}^{\infty} \delta^t U(C_t) = \mathbb{E}_0 \sum_{t=0}^{\infty} \delta^t \frac{C_t^{1-\sigma} - 1}{1-\sigma}, \tag{12}$$

where $\mathbb{E}_0$ denotes the expectation operator in the initial period and δ is the subjective discount factor. The sovereign finances consumption with the exogenous output and the issuance of unsecured long-term bonds, B_{t+1}, at price q_t. The bond structure follows Chatterjee and Eyigungor (2012): in each period, a fraction λ of outstanding bonds matures and a coupon η is due. Thus, the net issuance income is $q_t\,(B_{t+1} - (1-\lambda)B_t)$, while payments on maturing bonds and coupons amount to $(\lambda + (1-\lambda)\eta)B_t$. A similar and widely used long-maturity debt structure is in Hatchondo and Martinez (2009). Both types of long-maturity structures bring sovereign default models closer to the data by increasing the volatility of debt spreads and the average of debt-to-GDP ratios, largely due to inherent debt dilution incentives.

The sovereign chooses either to repay ($d = 0$) or default ($d = 1$) on its debts. If it repays, it retains a good credit record and achieves value V^r:

$$V^r(b, \tilde{\mathbf{s}}) = \max_{c>0,\, b'} \Big\{ U(c) + \delta \gamma^{1-\sigma} \mathbb{E}_{\tilde{\mathbf{s}}'|\tilde{\mathbf{s}}} V(b', \tilde{\mathbf{s}}') \Big\}, \tag{13}$$

[13] $\mathbf{P}_t \equiv \mathbb{E}\,[(\boldsymbol{\alpha}_t - \mathbf{a}_t)(\boldsymbol{\alpha}_t - \mathbf{a}_t)']$ evolves according to the *Riccati equation*: $\mathbf{P}_{t+1} = \mathbf{T}\mathbf{P}_t\mathbf{T}' - \mathbf{Z}\mathbf{P}_t\mathbf{Z}'(\mathbf{Z}\mathbf{P}_t\mathbf{Z}')^{-1}\mathbf{Z}\mathbf{P}_t\mathbf{T}' + \mathbf{R}\mathbf{Q}\mathbf{R}'$. We solve for the stationary $\mathbf{P}$ by iterating from an initial guess $\mathbf{P}_0$ until convergence (i.e., $|\mathbf{P}_{t+1} - \mathbf{P}_t| < 10^{-8}$).

where $\tilde{\mathbf{s}} \equiv [\tilde{\gamma}, \tilde{z}]$ are perceived shocks and $\mathbb{E}_{\tilde{\mathbf{s}}'|\tilde{\mathbf{s}}}$ is the conditional expectation over future beliefs. Here c and b are detrended consumption and debt.[14]

Bond issuance follows policy $b' = \mathcal{B}(b, \tilde{\mathbf{s}})$, subject to the budget constraint:

$$c = y(\tilde{\mathbf{s}}) + q(b', \tilde{\mathbf{s}}) \left[\tilde{\gamma} b' - (1-\lambda) b\right] - (\lambda + (1-\lambda)\eta) b, \tag{14}$$

where $q(b', \tilde{\mathbf{s}})$ is the price function. If the sovereign defaults and keeps a bad credit record, it obtains value V^d:

$$V^d(\tilde{\mathbf{s}}) = U((1-\psi) y(\tilde{\mathbf{s}})) + \delta \gamma^{1-\sigma} \mathbb{E}_{\tilde{\mathbf{s}}'|\tilde{\mathbf{s}}} \Big[(1-\mu) V^d(\tilde{\mathbf{s}}') + \mu V^r(\Phi(\tilde{\mathbf{s}}'), \tilde{\mathbf{s}}') \Big], \tag{15}$$

where $1-\mu$ is the probability that the sovereign remains in bad credit standing and cannot issue new bonds. Otherwise, the sovereign renegotiates and regains a good credit record with restructured debt $\Phi(\tilde{\mathbf{s}}')$. With a bad credit record, the sovereign suffers a proportional output loss on detrended output, $\psi y(\tilde{\mathbf{s}})$, hence $c = (1-\psi) y(\tilde{\mathbf{s}})$. The sovereign's default choice is:

$$V(b, \tilde{\mathbf{s}}) = \max_{d \in \{0,1\}} (1-d) V^r(b, \tilde{\mathbf{s}}) + d V^d(\tilde{\mathbf{s}}). \tag{16}$$

During renegotiation, the sovereign's threat point is the value of permanent autarky:

$$V^{aut}(\tilde{\mathbf{s}}) = U((1-\psi) y(\tilde{\mathbf{s}})) + \delta \gamma^{1-\sigma} \mathbb{E}_{\tilde{\mathbf{s}}'|\tilde{\mathbf{s}}} V^{aut}(\tilde{\mathbf{s}}'), \tag{17}$$

while the threat point for foreign creditors is zero recovery, $\phi = 0$. The sovereign's surplus is the difference between repaying the bonds after haircut ϕ, and the value of staying in autarky:

$$\Delta^s(\phi, \tilde{\mathbf{s}}) = V^r(\phi, \tilde{\mathbf{s}}) - V^{aut}(\tilde{\mathbf{s}}). \tag{18}$$

The surplus for creditors is the market value of restructured bonds:

$$\Delta^c(\phi, \tilde{\mathbf{s}}) = \Big[\lambda + (1-\lambda)(\eta + q(\phi', \tilde{\mathbf{s}}))\Big] \phi, \tag{19}$$

where $\phi' = \mathcal{B}(\phi, \tilde{\mathbf{s}})$ is the bond issuance after debt restructuring. Restructured bond ϕ is

[14] We detrend by perceived trend: $c_t = C_t / \tilde{\Gamma}_{t-1}$, $b_{t+1}\tilde{\gamma}_t = B_{t+1}/\tilde{\Gamma}_t \cdot (\tilde{\Gamma}_t / \tilde{\Gamma}_{t-1})$.

determined by a Nash Bargaining game as in Yue (2010) and Mihalache (2020):

$$\Phi(\tilde{\mathbf{s}}) = \arg\max_{\phi} \Big[\Delta^s(\phi, \tilde{\mathbf{s}})\Big]^{\alpha} \Big[\Delta^c(\phi, \tilde{\mathbf{s}})\Big]^{1-\alpha}, \quad \Delta^s \geq 0 \text{ and } \Delta^c \geq 0, \tag{20}$$

where α governs the sovereign's bargaining power. The recovery rate from such a restructuring is $\Phi(\tilde{\mathbf{s}})/b$. Most historical sovereign default episodes involve non-trivial haircuts on outstanding debts. During the 2010s Eurozone debt crisis, the 2012 Greek default involved an approximately 40% haircut (Arellano and Bai, 2017).

Foreign creditors price new and outstanding bonds by accounting for default probabilities and recovery values:

$$q(b', \tilde{\mathbf{s}}) = \frac{1}{1+r^*} \mathbb{E}_{\tilde{\mathbf{s}}'|\tilde{\mathbf{s}}} \Big\{ (1 - d(b', \tilde{\mathbf{s}}')) \Big[\lambda + (1-\lambda)(\eta + q(b'', \tilde{\mathbf{s}}')) \Big] + d(b', \tilde{\mathbf{s}}') q^d(b'', \tilde{\mathbf{s}}') \Big\}, \tag{21}$$

where r^* is a world risk-free rate, q^d is the price (recovery rate) for the restructured bonds:

$$q^d(b', \tilde{\mathbf{s}}) = \frac{1}{1+r^*} \mathbb{E}_{\tilde{\mathbf{s}}'|\tilde{\mathbf{s}}} \Big\{ (1-\mu) q^d(b', \tilde{\mathbf{s}}') + \mu \frac{\Delta^c(\phi, \tilde{\mathbf{s}}')}{b} \Big\}, \tag{22}$$

where $\phi = \Phi(\tilde{\mathbf{s}}')$ is the restructured bonds after renegotiation. The spread is then

$$rs(b', \tilde{\mathbf{s}}) = \frac{\lambda + (1-\lambda)\eta}{q(b', \tilde{\mathbf{s}})} - \lambda - r^* \tag{23}$$

where the numerator is the average coupon flow per unit of face value, dividing by $q(b', \tilde{\mathbf{s}})$ yields the implied yield, and subtracting $(\lambda + r^*)$ benchmarks it against the risk-free rate.

Definition 1 (Equilibrium in the II model)**.** Given outstanding bonds b, perceived states $\tilde{\mathbf{s}} = [\tilde{z}, \tilde{\gamma}]$, and rational expectations about their evolution $\mathbb{E}_{\tilde{\mathbf{s}}'|\tilde{\mathbf{s}}}$, a recursive equilibrium consists of optimal policy functions for default d, consumption c, and bond issuance $\mathcal{B}$, associated value functions V^r, V^d, V, V^{aut}, and price schedules q, q^d, such that:

1. Given $q(b', \tilde{\mathbf{s}})$, $V^r(b, \tilde{\mathbf{s}})$ yields the optimal debt issuance policy $b' = \mathcal{B}(b, \tilde{\mathbf{s}})$.
2. $\mathcal{B}(b, \tilde{\mathbf{s}})$ and the perceived state $\tilde{\mathbf{s}}$ determine $V^d(\tilde{\mathbf{s}})$, $V(b, \tilde{\mathbf{s}})$, $V^{aut}(\tilde{\mathbf{s}})$, the default decision $d(b, \tilde{\mathbf{s}})$, and the renegotiation outcome $\Phi(\tilde{\mathbf{s}})$.
3. Bond prices satisfy the risk-neutral pricing conditions (21) and (22).

4. Optimal consumption c satisfies (14) when the sovereign repays or $c = (1-\psi)y(\tilde{\mathbf{s}})$ when it defaults, given policies and states.

Full-information (FI) RE model. The FI model is a special case of the II model where agents observe the true (z_t, γ_t) directly. Its expectation operator $\mathbb{E}_{\mathbf{s}'|\mathbf{s}}$ reflects the orthogonal transition laws of trend and cycle defined in equations (6) and (4). The recursive structure of the dynamic programming problem, bond pricing, and default/renegotiation are otherwise identical to the II model.

3.4 Model computation

The learning mechanism in the II model applies exclusively to the exogenous variables $[\tilde{\gamma}_t, \tilde{z}_t]$, which evolve according to the realization of true shocks $[\gamma_t, z_t]$, the noise shock n_t, and the Bayesian learning rule in equation (11). From the agents' perspective, the transition probability $\Pr(\tilde{\gamma}_{t+1}, \tilde{z}_{t+1} \mid \tilde{\gamma}_t, \tilde{z}_t)$ is treated as given when making decisions. We approximate this transition probability using a discretized transition matrix $\mathbb{E}_{\tilde{\mathbf{s}}'|\tilde{\mathbf{s}}}$, which is constructed by simulating sequences of $\tilde{\gamma}_t$ and $\tilde{z}_t$ based on random realizations of shocks z_t, γ_t, and n_t, according to the learning rule (11). As a result, the probability of transitioning from a given grid point $\tilde{z}_t$ $(\tilde{\gamma}_t)$ to a new grid point $\tilde{z}_{t+1}$ $(\tilde{\gamma}_{t+1})$ is related not only to its own current value but also to the current value of $\tilde{\gamma}_t$ $(\tilde{z}_t)$. For example, low values of $\tilde{\gamma}_t$ are more likely to be observed alongside low $\tilde{z}_t$, and rarely with high $\tilde{z}_t$, and vice versa.

In the numerical implementation, each exogenous state is discretized into 35 equally spaced grid points covering a range of ± 4.2 standard deviations from its unconditional mean. For the probability transition matrix $\mathbb{E}_{\mathbf{s}'|\mathbf{s}}$ in the FI model, we draw the distributions of the exogenous shocks γ_t and z_t independently based on their respective true laws of motion, i.e., equations (6) and (4).

Incorporating long-term debt pricing via equations (21) introduces well-known convergence challenges in value function iteration (Chatterjee and Eyigungor, 2012). To address this, we introduce taste shocks into all discrete bond choices b' and default decisions d. Similar to the i.i.d. income shock m used in Chatterjee and Eyigungor (2012), these taste shocks smooth the right-hand sides of the pricing equations, thereby avoiding large oscillations during iteration and hence facilitating equilibrium computation. This smoothing approach has become stan-

dard in sovereign default models with long-maturity debts and discrete debt choices, including Gordon (2019), Mihalache (2020), and Dvorkin et al. (2021).

Taking the II model as an example, the probability of choosing bond policy b' is:

$$\mathbb{P}(b' = i|b, \tilde{\mathbf{s}}) = \frac{\exp\Big[(\mathcal{W}(b, \tilde{\mathbf{s}}, i) - \mathcal{W}^*(b, \tilde{\mathbf{s}}))/\sigma_b\Big]}{\sum_{\tilde{i}} \exp\Big[(\mathcal{W}(b, \tilde{\mathbf{s}}, \tilde{i}) - \mathcal{W}^*(b, \tilde{\mathbf{s}}))/\sigma_b\Big]}, \tag{24}$$

where $\mathcal{W}(b, \tilde{\mathbf{s}}, b') = U(c) + \delta \mathbb{E}_{\tilde{\mathbf{s}}'|\tilde{\mathbf{s}}} V(b', \tilde{\mathbf{s}}')$ is the value of repayment and $\mathcal{W}^*(b, \tilde{\mathbf{s}})$ is the maximum across candidate policies. The non-default probability is:

$$\mathbb{P}(d = 0|b, \tilde{\mathbf{s}}) = \frac{\exp\Big[V^r(b, \tilde{\mathbf{s}})/\sigma_d\Big]}{\exp\Big[V^d(\tilde{\mathbf{s}})/\sigma_d\Big] + \exp\Big[V^r(b, \tilde{\mathbf{s}})/\sigma_d\Big]}. \tag{25}$$

Debt renegotiation outcomes follow:

$$\mathbb{P}(\phi = i|\tilde{\mathbf{s}}) = \frac{\exp\left[(\oplus(i, \tilde{\mathbf{s}}) - \Phi(\tilde{\mathbf{s}}))/\sigma_\phi\right]}{\sum_{\tilde{i}} \exp\Big[(\oplus(\tilde{i}, \tilde{\mathbf{s}}) - \Phi(\tilde{\mathbf{s}}))/\sigma_\phi\Big]}, \tag{26}$$

with $\oplus(i, \tilde{\mathbf{s}}) = [\Delta^s(i, \tilde{\mathbf{s}})]^\alpha [\Delta^c(i, \tilde{\mathbf{s}})]^{1-\alpha}$. Positive values of σ_b, σ_d, and σ_ϕ facilitate convergence of the debt price mapping. In implementation, b is discretized into 200 equally spaced grid points over $[0.35\%, 1.35\%]$ of the steady state of detrened output $\bar{y}$ (normalized to 1), and simulated paths remain within this range (Figure 3). We set $\sigma_b = \sigma_d = \sigma_\phi = 0.0005$, which yields convergence within 1,000 iterations while keeping the influence on model predictions minimal.

We note that while introducing taste shocks facilitates the computation of a Markov equilibrium, to the best of our knowledge it does not guarantee uniqueness. Under the calibration described in the next section, the equilibrium we compute exhibits defaults, positive average spreads, and a borrowing policy that occasionally exits the non-default region. These features align with the *borrowing equilibrium* in the Chatterjee and Eyigungor (2012) long-maturity debt framework, as discussed in Aguiar and Amador (2020), and are consistent with most Markov equilibria found in quantitative sovereign default models calibrated to match empirically relevant spread moments.[15]

[15]Chatterjee and Eyigungor (2012) acknowledge while they obtain a unique solution, they cannot prove the

Finally, the choice probability structure in equations (24), (25), and (26) resembles discrete-choice functional forms commonly used in behavioral macroeconomic models (e.g., Brock and Hommes, 1997; De Grauwe and Ji, 2019). In that literature, probabilistic decision rules are typically employed to model agents' switching across competing forecasting rules based on their relative performance, a mechanism that can generate endogenous business cycles as well as fat-tailed and asymmetric distributions. Although our model adopts a similar mathematical structure and likewise produces left-skewed and fat-tailed distributions of outstanding debt (see Figure 3), it does not feature endogenous regime switching driven by belief updating across alternative forecasting rules. Instead, stochasticity in our framework arises from the interaction of exogenous fundamental shocks and forward-looking beliefs about them, combined with endogenous decisions governed by equations (24), (25), and (26).

4 Calibration

We calibrate the benchmark Imperfect Information (II) model to annual Portuguese data, 1999-2019. Portugal is an interesting case for three reasons. First, Portugal is a small open economy that has historically been more vulnerable to sovereign default risk than larger GIIPS countries, including a documented default in 1892. Second, during the euro area crisis, its 10-year government bond yield peaked at 13%, indicating substantially higher default risk than Spain or Italy (with the peak lower than 5%). Third, as noted by Paluszynski (2023), the Portuguese crisis episode was relatively "clean", without the systemic banking crisis of Ireland or the large-scale ECB interventions—such as Outright Monetary Transactions (OMT)–that coincided with the crisis peaks in Italy and Spain.[16]

uniqueness of equilibrium in their long-maturity debt framework. Recent studies, including Aguiar and Amador (2020), find multiple equilibria is possible in Chatterjee and Eyigungor (2012). By altering the curvature of utility, Stangebye (2020) shows different initial guesses for the bond price schedule can lead to multiplicity. He argues in an alternative framework (e.g., Hatchondo and Martinez, 2009), which solves the model via backward induction from a finite-horizon problem, can only yield a single equilibrium. For models with one-period bonds, Auclert and Rognlie (2016) prove the uniqueness of equilibrium. Within our framework, we tested alternative initial guesses and found that the algorithm consistently converged to virtually the same equilibrium, with sup-norm differences in the bond price schedule below 10^{-11}.

[16]As a robustness check, Online Appendix D reports results for the II model calibrated to Spain. The learning mechanism continues to generate a negative correlation between sovereign spreads rs_t and perceived trend growth $\tilde{\gamma}_t$, though the lower mean and volatility of Spanish spreads (henceforth lower default risk) dampen the magnitude of this relationship. We expect similar results for other economies that have experienced substantial sovereign default risk. Greece is excluded due to missing IMF potential growth estimates (2003–2008) and major structural breaks in fiscal policy following its 2012 default.

4.1 Calibrating model parameters and the belief updating process

Regarding the learning mechanism in equation (11), we set the persistence parameter $\rho_n = 0.9$, following Uribe and Schmitt-Grohé (2017) Chapter 5. For the cyclical shock z_t, we set $\rho_z = 0.9$, as in much of the sovereign default literature to introduce realistic spreads. The innovation standard deviation σ_z is chosen so that simulated GDP growth, $\Delta \log(Y_t) = \tilde{z}_t - \tilde{z}_{t-1} + \tilde{\gamma}_t$, matches the observed variance of annual GDP growth from Eurostat, given the trend growth parameters.

The trend process parameters $[\rho_\gamma, \sigma_\gamma]$ are set so that the persistence and variance of simulated $\tilde{\gamma}_t$ match real-time potential growth estimates from the EEF. Together with σ_z and σ_γ, the noise standard deviation σ_n is adjusted to match two statistics from simulation: (i) the correlation between beliefs about trend and cycle $corr(\tilde{\gamma}_t, \tilde{z}_t)$, and (ii) the autocorrelation coefficient of the potential growth estimation errors $\tilde{\gamma}_t^{err} = \tilde{\gamma}_t - \gamma_t$. The parameters that do not depend on model simulations are reported in Table 4, while the simulation-calibrated parameters are reported in Table 5.

Table 4: Parameters independent of II model simulation

Description	Parameters	Value	Source
Cyclical growth persistence	ρ_z	0.9	Aguiar and Gopinath (2006)
Trend growth persistence	ρ_γ	0.88	EEF Portugese data
Trend growth stan. dev.	σ_γ	0.85%	EEF Portugese data
Average growth rate	$\overline{\gamma}$	1%	Portugese data
Noise process persistence	ρ_n	0.9	Uribe and Schmitt-Grohé (2017)
Risk aversion	σ	2	Chatterjee and Eyigungor (2012)
Reentry probability	μ	15.4%	Cruces and Trebesch (2013)
Risk-free rate	r^*	4%	German data
Average maturity	$1/\lambda$	5.0	Paluszynski (2023)

Notes: Calibration of parameters that does not require solving or simulating the sovereign default model. The model is in discrete time and annual frequency.

For the FI model, the trend parameters are set to $\rho_\gamma = 0.9144$ and $\sigma_\gamma = 0.18\%$ from the HP-filtered trend component of Portuguese log GDP, with $\sigma_z = 3.1\%$ to match observed GDP annual growth volatility. To ensure comparability, all other parameters for the output and sovereign default structures are identical to those in the benchmark II model.

Table 5: Parameters calibrated to targeted data moments

Description of parameters	Parameters	Value
Std of ε_t^z	σ_z	4.1%
Std of ε_t^n	σ_n	1.5%
Bargaining power in renegotiation	α	0.605
Subjective discount rate	δ	0.78
Output loss in default	ψ	10.25%
Coupon rate of bond	η	5.8%
Lower bound of price	$\underline{q}$	0.5
Targeted data moments	Data	II Model
Std of $\Delta \log(Y_t)$	3.2%	3.2%
Autocorr. coefficient of $\tilde{\gamma}_t$	0.895	0.897
Std of innovations to $\tilde{\gamma}_t$	0.55%	0.56%
Correlation between $\tilde{\gamma}_t$ and $\tilde{z}_t$	0.61	0.73
Autocorr. coefficient of $\tilde{\gamma}_t^{err}$	0.72	0.67
Mean spreads $\mathbb{E}(rs_t)$	1.91%	1.90%
Gov debt-to-GDP $\mathbb{E}(B_t/Y_t)$	96%	90%
Mean haircut $\mathbb{E}(\Phi(\mathbf{s})/b)$	40%	40%

Notes: Statistics are based on annual data from 1999 to 2019 and simulated periods with good credit standing. rs_t denotes sovereign spreads, defined as the yield differential between Portuguese and German 10-year government bonds. Trend estimates are real-time potential GDP growth rates. $\tilde{\gamma}_t^{err} = \tilde{\gamma}_t - \gamma_t$, as defined in Table 1.

In the II model, the implied signal-to-noise ratio for trend growth is:

$$\frac{\sigma_\gamma}{\sqrt{1-\rho_\gamma^2}} \Bigg/ \frac{\sigma_n}{\sqrt{1-\rho_n^2}} = 0.52, \tag{27}$$

and the relative importance of trend shocks is:

$$V = \frac{\sigma_\gamma^2/(1-\rho_\gamma^2)}{2\sigma_z^2/(1+\rho_z) + \sigma_\gamma^2/(1-\rho_\gamma^2)} = 0.15. \tag{28}$$

Thus, trend shocks account for a modest share of aggregate output fluctuations, consistent with Boz et al. (2011) (signal-to-noise of 0.58 and $V = 0.23$ for developed economies). The FI model yields $V = 0.02$, in line with Garcia-Cicco et al. (2010), who find trend shocks explain only 2.4% of total factor productivity variation in a full-information model that accounts for financial frictions like the country risk premia.

4.2 Calibrating the sovereign default structure

The reentry probability $\mu = 0.154$ implies an average 6.5-year exclusion after default, in line with sovereign default events with haircuts above 30% reported in Cruces and Trebesch (2013). The annual coupon rate $\eta = 5.9\%$ ensures bonds with an average 1.9% spread and a 4% risk-free rate trade near par, consistent with the method in Chatterjee and Eyigungor (2012). The average maturity $1/\lambda = 5.0$ matches Portuguese debt maturity (1996–2010) reported in Paluszynski (2023). The subjective discount factor $\delta = 0.78$, output loss in default $\psi = 10.25\%$, and the debt renegotiation bargaining power parameter $\alpha = 0.605$ jointly match: (i) the average sovereign bond spreads 1.9%, (ii) the average government debt-to-GDP ratio 90%, and (iii) a reference average haircut of 40% reflecting Greece's 2012 debt restructuring (Arellano and Bai, 2017).[17] As shown in the lower panel of Table 5, the model successfully replicates key empirical moments.

Debt dilution, introduced by the long-maturity debt structure, and a positive recovery rate give the government strong incentives to issue large amounts of debt, enabling a sharp rise in consumption just before defaulting in the next period. Following Hatchondo et al. (2016), we avoid this problem by imposing a debt price floor $\underline{q} = 0.5$, corresponding to a 25% peak spread, roughly the maximum observed for GIIPS countries in 2012 Q2 (Greek default). This floor rarely binds in simulations.

5 Results

5.1 Simulated moments

Table 6 reports key statistics from the data and model simulations. We simulate both II and FI models for 300 independent chains of 4,000 periods each and compute statistics after excluding periods of default and a bad credit record (i.e., after default and before reentry). The reported moments are the medians across chains.

Table 6 shows that the II model replicates key moments more closely than the FI model.[18]

[17] The assumption of impatient agents that a low δ indicates is common in sovereign default calibrations. While Portugal avoided default, the Greek debt restructuring offers a relevant reference point for how markets priced other sovereign debts during the crisis.

[18] As documented in the literature, the proportional output loss function (Equation 15) tends to underpredict $\sigma(rs_t)$. Nonlinear loss functions, such as those in Chatterjee and Eyigungor (2012), can address this issue.

Table 6: Main moments from simulation and Portuguese data

Statistics	Data	II Model	FI Model
$\mathbb{E}(rs_t)$	1.91	1.90	0.70
$\mathbb{E}(B_t/Y_t)$	96%	90%	117%
$\sigma(rs_t)$	2.44	0.37	0.10
$\sigma(c_t)/\sigma(y_t)$	1.02	1.14	1.20
$corr(y_t, c_t)$	0.92	0.81	0.77
$corr(rs_t, y_t)$	-0.52	-0.35	-0.37
$corr(rs_t, c_t)$	-0.57	-0.05	-0.01
$corr(rs_t, B_t/Y_t)$	0.67	0.63	0.56
$\hat{\rho}(\tilde{\gamma}_t^{err})$	0.72	0.67	n.a.

Notes: y and c data are log-transformed and HP-detrended. $\tilde{\gamma}$ denote perceived trend growth (real-time potential growth estimates) in the II model (data); in the FI model, it equals the true trend shocks. $\tilde{\gamma}_t^{err}$ is the deviation between $\tilde{\gamma}$ and true trend growth (HP-filtered trend growth of GDP in data). Portuguese data: annual, 1999–2019. Simulated periods are restricted to those with good credit standing.

By contrast, the FI model generates spreads that are too low, a debt-to-GDP ratio that is too high, and spreads that are overly stable. The II model's improvement comes from the learning mechanism, which links perceived trend growth rates with cycles, increasing the volatility of trend growth beliefs. When persistent declines in trend growth are believed to be more frequent, default risk rises, and foreign creditors demand higher spreads to break even on expected returns. This forces the sovereign to sustain, on average, a lower level of outstanding debt. As Figure 3 shows, the II model produces a lower and more dispersed debt distribution than the FI model.[19]

The II model also better matches the strong correlations between spreads and perceived trend growth. We calculate these correlation coefficients around spread peaks because low-risk periods, when spreads respond little to shocks and trend growth is often overestimated, dilute the relationship in full-sample statistics (Table 6). As shown in Table 7, in the II model, near-crisis correlations reach $corr(rs_t, \tilde{\gamma}_t) = -0.42$ and $corr(rs_t, \tilde{z}_t) = -0.42$, compared with -0.13 and -0.11 in the full sample. By contrast, in the FI model, the correlation between spreads and trend growth is still weak ($corr(rs_t, \gamma_t) = -0.13$) near crises, and even lower than in the

However, empirical evidence on how output losses split between trend and cyclical components remains limited.

[19]Many of the simulated b_t values around $b_t/\bar{y} = 0.6$ in Panel (a) of Figure 3 come from renegotiation outcomes: the sovereign receives a haircut, so these restructured debts are significantly lower than the outstanding debts before default.

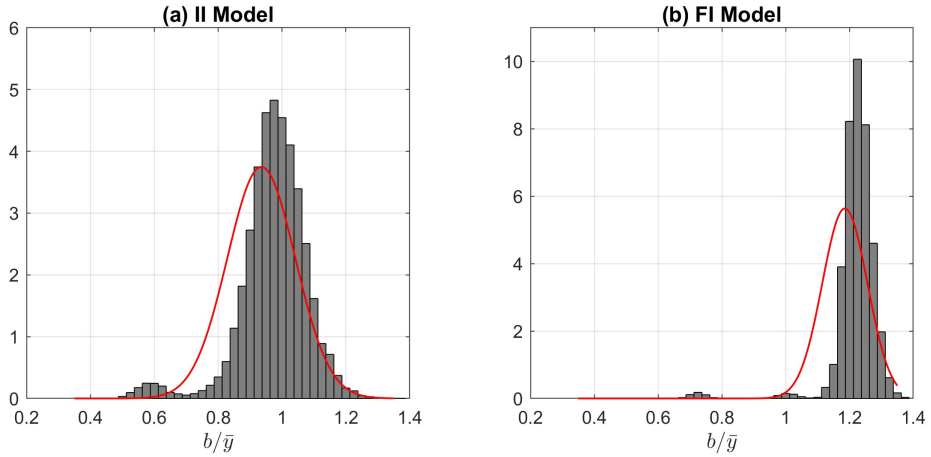

Figure 3: Debt distributions from II and FI models during simulated periods with good credit standing. Red curves are fitted normal densities using the simulated mean and standard deviation.

Table 7: Selected statistics around crisis periods vs. full sample

		II Model		FI Model	
Statistics	Data	Full sample	Near crises	Full sample	Near crises
$\mathbb{E}(rs_t)$	1.91	1.90	2.01	0.69	0.72
$\sigma(rs_t)$	2.44	0.37	2.41	0.10	0.98
$corr(rs_t, \tilde{z}_t)$	-0.42	-0.13	-0.42	-0.31	-0.39
$corr(rs_t, \tilde{\gamma}_t)$	-0.71	-0.11	-0.42	0.02	-0.13
$corr(\tilde{\gamma}_t, \tilde{z}_t)$	0.61	0.72	0.75	-0.04	-0.01
$corr(rs_t, y_t)$	-0.52	-0.35	-0.58	-0.37	-0.41
$corr(rs_t, c_t)$	-0.57	-0.07	-0.44	-0.01	-0.40

Notes: "Near crises" includes non-default periods centered on spread peaks (13 years before to 7 years after) where spreads exceed the simulated 95th percentile. "Full sample" includes all non-default periods.

full sample ($corr(rs_t, \gamma_t) = 0.02$). These differences highlight the role of substantial default risk in explaining the observed link between long-run growth beliefs and sovereign spreads.

The small correlation $corr(rs_t, c_t)$ in Table 6 arises because when default risk is low, borrowing can smooth consumption without significantly steepening the spread curve. When the curve is steep, as around spread peaks (Table 7), the II model yields $corr(rs_t, c_t) = -0.44$ while the FI model gives -0.40.

The II model also generates systematic trend growth estimation errors around sovereign spread peaks. In Figure 4 panel (a), trend growth is overestimated before the peak (II trajectory above FI) and underestimated after the peak, in line with the data (Figure 1). The simulated boom–bust cycles in output and consumption (panels (c) and (d)), the persistent

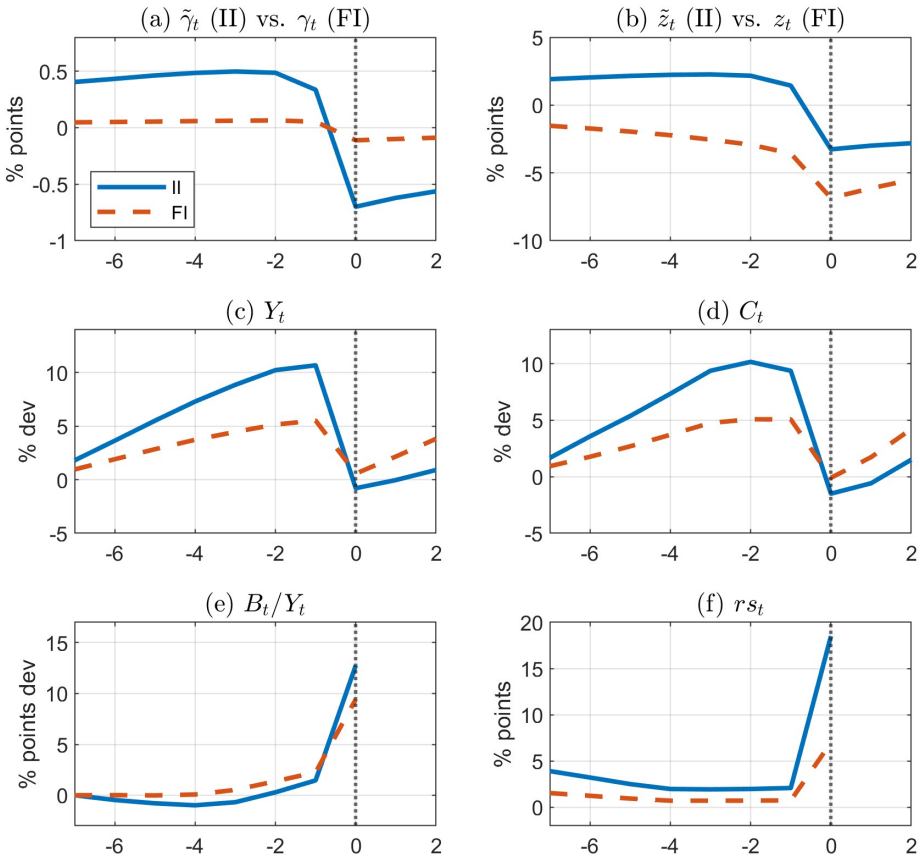

Figure 4: Typical episodes of spread peaks from simulated II and FI models (mean trajectories around spread peaks in 1 million simulated periods, without a bad credit record) where spreads exceed the 95th percentile. Period 0 marks the spread peak, while period -1 (on the horizontal axis) marks one year before it. Y and C denote percentage deviations relative to their levels at period -8. γ_t ($\tilde{\gamma}_t$) denotes (beliefs about) deviation in trend growth from the unconditional mean.

rise in the debt-to-GDP ratio (panel (e)), and the sharp spread increase (panel (f)) resemble Portuguese episodes.[20] Compared to the FI model, the II model generates a larger peak in spreads and a slightly greater buildup of debt, which together reduce disposable income. This joint shift in trend growth beliefs and debt dynamics explains the divergence in macro outcomes: before the peak, output is about 5% higher in the II model compared to the FI model, but about 2% lower afterward; consumption follows a similar pattern, being roughly 5% higher before the peak and 2% lower afterward.

[20]In the data, the peak-to-trough declines were 8% in output and 10% in consumption relative to 2004, the debt-to-GDP ratio rose by 50 percentage points, and spreads surged by 9% before Portugal's 10-year government bond spread peak in 2012.

5.2 Nonlinearity analysis

Does the II model produce a nonlinear relationship between sovereign spreads and trend growth estimates, as suggested by the empirical evidence? To test this, we estimate the following nonlinear regression using simulated data from both the II and FI models, paralleling equation (1):

$$rs_t = \beta_0^{sim} + \beta_{\tilde{\gamma},l}^{sim} I_t^l \tilde{\gamma}_t + \beta_{\tilde{\gamma},m}^{sim} I_t^m \tilde{\gamma}_t + \beta_{\tilde{\gamma},h}^{sim} I_t^h \tilde{\gamma}_t + \beta_b^{sim} \Delta(b_t/y_t) + \beta_{\tilde{z}}^{sim} \tilde{z}_t + u_t^{sim}, \tag{29}$$

and the corresponding linear specification, parallelizing (2):

$$rs_t = \bar{\beta}_0^{sim} + \bar{\beta}_{\tilde{\gamma}}^{sim} \tilde{\gamma}_t + \bar{\beta}_b^{sim} \Delta(b_t/y_t) + \bar{\beta}_{\tilde{z}}^{sim} \tilde{z}_t + \bar{u}_t^{sim}. \tag{30}$$

Here, superscript *sim* indicates regressions are estimated on simulated data. Both u_t^{sim} and $\bar{u}_t^{sim}$ are i.i.d. error terms. State variables b_t and $\tilde{z}_t$ (z_t in the FI model) are included as controls. Consistent with the empirical specifications in (2) and (1), we use the first difference of the simulated debt-to-GDP ratio, $\Delta(b_t/y_t)$, as a control.

Table 8 reports the estimated coefficients by trend growth regime. In the II model, spreads are far more sensitive to low values of $\tilde{\gamma}_t$ (about -225 bps) than to medium or high values, closely mirroring the empirical estimates from EEF and WEO data (Table 3). By contrast, the FI model's coefficients vary little across regimes, showing no comparable state dependence. This difference highlights the role of imperfect information in generating the observed nonlinear link between spreads and long-run growth expectations.

5.3 Impulse response functions

To examine the model's dynamics, we compute generalized impulse response functions (IRFs) using the simulation-based approach of Koop et al. (1996) and Arellano et al. (2018). We simulate two groups of 300,000 independent paths, each with 641 periods.

The first group consists of *shocked paths*. From periods 1–600, z_t, γ_t, and n_t evolve according to their respective Markov chains. At period 601 (normalized to period 0 in the IRFs), we apply an additional shock to either z_t or γ_t, while the other exogenous variables continue to evolve undisturbed. From period 601 onward, beliefs $\tilde{z}_t$ and $\tilde{\gamma}_t$ are updated via the Bayesian

Table 8: Estimation results by growth regime based on II and FI model simulations

	II Model	FI Model
Linear regression (30)		
$\tilde{\gamma}_t$	-65.6^{***}	-61.7^{***}
	(0.47)	(0.48)
R^2	0.15	0.10
Nonlinear regression (29)		
Low $\tilde{\gamma}_t$	-224.8^{***}	-107.9^{***}
	(1.36)	(1.45)
Medium $\tilde{\gamma}_t$	-71.6^{***}	-90.2^{***}
	(0.71)	(0.80)
High $\tilde{\gamma}_t$	-43.6^{***}	-70.6^{***}
	(0.50)	(0.58)
R^2	0.16	0.11

Notes: Regression coefficients report the change in sovereign spreads (basis points) from a one-percentage-point change in perceived trend growth ($\tilde{\gamma}_t$ in the II model, γ_t in the FI model). Each regression uses approximately 3.5 million simulated observations per model, excluding periods with a bad credit record. Control variables $\Delta(b_t/y_t)$ and $\tilde{z}_t$ (z_t in FI) are included but not shown; both are significant with $\hat{\beta}_{\tilde{z}}^{sim} < 0$, $\hat{\tilde{\beta}}_{\tilde{z}}^{sim} < 0$, $\hat{\beta}_b^{sim} > 0$, and $\hat{\tilde{\beta}}_b^{sim} > 0$. Regimes are defined using the 25th and 75th percentiles of $\tilde{\gamma}_t$ (II model) or γ_t (FI model): II model: low $< 0.37\%$, medium $= 0.37$–1.93%, high $> 1.93\%$. FI model: low $< 0.78\%$, medium $= 0.78$–1.32%, high $> 1.32\%$. Standard errors in parentheses. *** denotes p-value below 0.01, ** denotes p-value below 0.05.

learning rule (11), and endogenous variables evolve according to the policy rules. The second group consists of *unshocked paths*, which are identical to the shocked paths except that no additional shock is applied at period 601.

Figures 5 and 6 display IRFs for the imperfect information (II, solid blue) and full information (FI, dashed red) models. Periods before 600 are discarded, and period 601 is normalized to period 1 on the horizontal axis. Paths with bad credit records at period 600 are excluded from the IRF calculation. For trending variables (e.g., output, consumption), IRFs represent average percentage deviations from the unshocked paths; for stationary variables, they represent percentage-point differences relative to the unshocked paths.

5.3.1 Negative trend shock

Figure 5 shows IRFs following a -50% standard deviation trend shock. In the II model, agents revise $\tilde{\gamma}_t$ downward (panel (f)) but also attribute part of the shock to a persistent slowdown in

the cycle (panel (e)). Recall that agents cannot observe γ_t directly, but only a noisy signal s_t. Because the signal is highly imprecise, agents: (i) adjust trend beliefs gradually, generating a hump-shaped response, and (ii) initially ascribe most of the output decline to the cycle, expecting recovery since they know the true cycle z_t is mean-reverting. When Y_t continues falling, however, they must further revise $\tilde{z}_t$ downward. As a result, the II model generates a prolonged decline in both perceived trend and cyclical components, leading to a deeper and more persistent output contraction (panel (b)): the trough is roughly 0.8 percentage points deeper than in the FI model, and the recovery is slower by about five years.

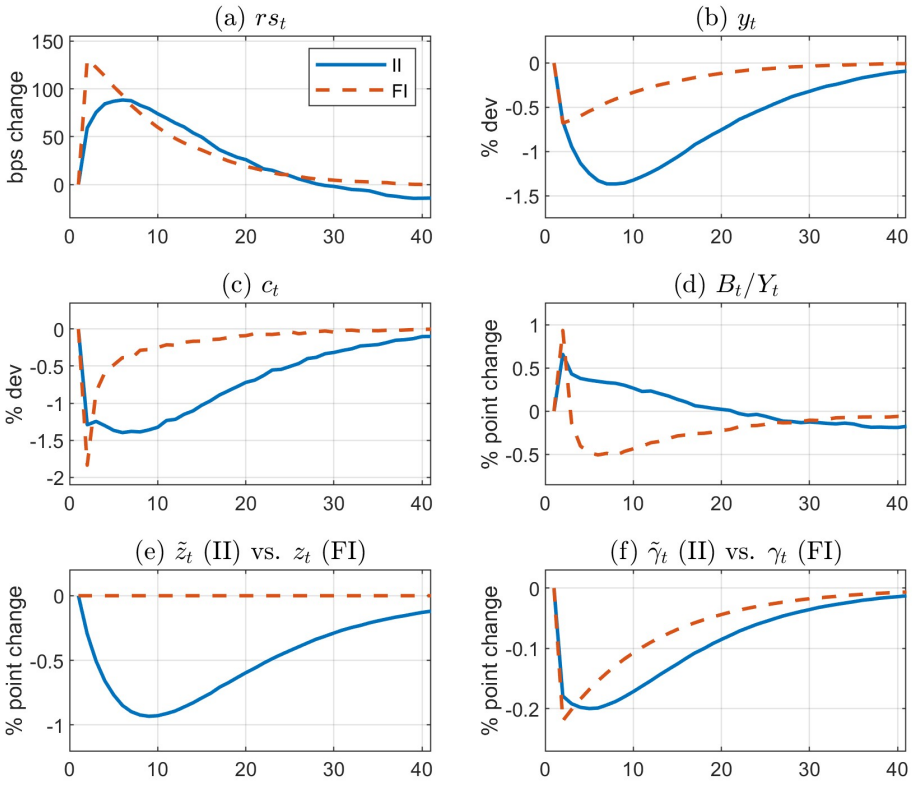

Figure 5: Generalized IRFs to a negative shock to the true trend growth process. For each model, the shock magnitude equals 50% of the standard deviation of its own underlying trend process.

The downward revision in $\tilde{z}_t$ introduces "cyclical effects" into the dynamics. Because much of the downturn is regarded as temporary, foreign creditors raise the risk premium only modestly compared to the FI model (panel (a)), which encourages the sovereign to increase the debt-to-GDP ratio (panel (d)) to smooth consumption. This rise in indebtedness, in turn, contributes to a more persistent increase in spreads. In the FI model, knowing the shock is

purely to trend growth, creditors anticipate a sharper deterioration in long-term repayment capacity and respond by charging higher spreads immediately. Facing a steeper yield curve, the sovereign deleverages more aggressively, reflecting "trend effects".

Finally, consumption dynamics (panel (c)) are jointly shaped by output and borrowing effects. In both models, consumption c_t falls on impact. In the II model, the hump-shaped and larger expected decline in output drives a gradual fall and slower recovery. Moreover, the associated rise in the debt-to-GDP ratio and the smaller fall in bond prices (the inverse of spreads) allow a milder initial contraction in c_t. In the FI model, deleveraging reduces consumption more sharply at first, about 0.6 percentage points more than in the II model, but the quicker output recovery supports a faster rebound, so that ten periods after the shock, FI consumption is roughly 1 percentage point higher than in the II path.

5.3.2 Negative cyclical shock

Upon receiving a -50% standard deviation z_t shock (Figure 6), the learning rule (11) leads agents to attribute part of the shock to adjustments in trend growth beliefs ($\tilde{\gamma}_t$). This results in an immediate downward revision of $\tilde{\gamma}_t$ (panel (f)), followed by a rebound that overshoots its pre-shock level after about ten periods. Meanwhile, $\tilde{z}_t$ falls by less than z_t (panel (e)), producing a smaller and shorter-lived decline in output y_t (panel (b)), roughly one percentage point milder than in the FI model.

Here, the learning mechanism introduces a "trend effect" into a cycle shock. Although $\tilde{z}_t$ is above z_t, bond spreads are more sensitive to long-term repayment capacity, which depends critically on $\tilde{\gamma}_t$.[21] As a result, the II model generates higher initial spreads than the FI model (panel (a)). As $\tilde{\gamma}_t$ rebounds above its pre-shock level in the longer run, spreads in the II model fall below those in the FI model.

Because trend growth is believed to slowdown, and the perceived reduction in cyclical growth is milder, the sovereign in the II model borrows less, raising the debt-to-GDP ratio by less than in the FI model (panel (d)). Combined with an expected faster cyclical recovery and an overshoot in trend growth, this moderate borrowing path contributes to lower long-term spreads in the II model (panel (a)).

In the early periods, however, lower bond issuance at lower prices limits external financing

[21] We discuss the sensitivity of spreads to different output shocks in the next section.

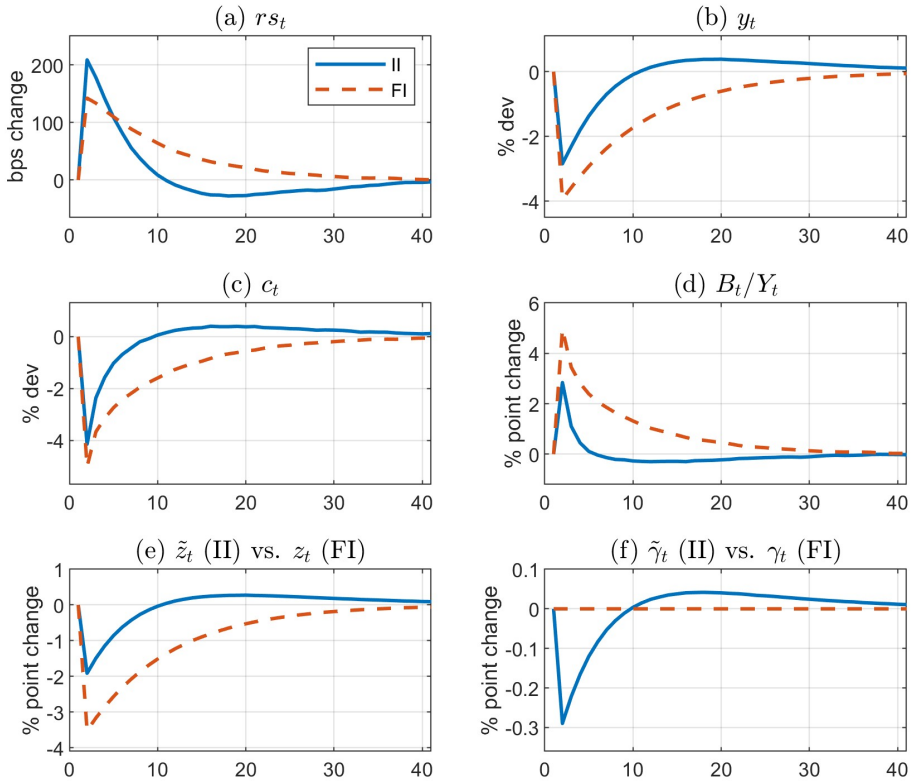

Figure 6: Generalized IRFs to a negative shock to the true cyclical growth process. For each model, the shock magnitude equals 50% of the standard deviation of its own underlying cycle process.

for consumption in the II model. Thus, despite a milder output contraction, consumption initially falls by a similar magnitude in both models (around 4%). Over the medium run, y_t and B_t/Y_t in the II model converge faster, leaving consumption roughly 1.5 percentage points higher than in the FI model.

5.4 The mechanism generating a nonlinear relationship

The mechanism illustrated by the IRFs above explains how the model reproduces Evidence 1 and the negative relationship between real-time estimates of potential GDP growth and sovereign debt spreads (Evidence 2(i)). This section focuses on the mechanism generating the nonlinearity documented in Evidence 2(ii).

In the FI model, trend and cyclical components of output are independent, with the trend accounting for only 1.5% of output growth variance. Both negative z_t and γ_t shocks can raise spreads, but z_t shocks are more likely to drive peaks due to their larger role in business

cycle fluctuations. Since z_t shocks are uncorrelated with γ_t shocks, the link between spreads and trend growth is weak (Table 7). By contrast, in the II model, learning generates strong comovement between $\tilde{z}_t$ and $\tilde{\gamma}_t$. This misperception leads to underestimated trend growth during cyclical downturns, amplifying long-term repayment concerns and strengthening the negative correlation between perceived trend and spreads.

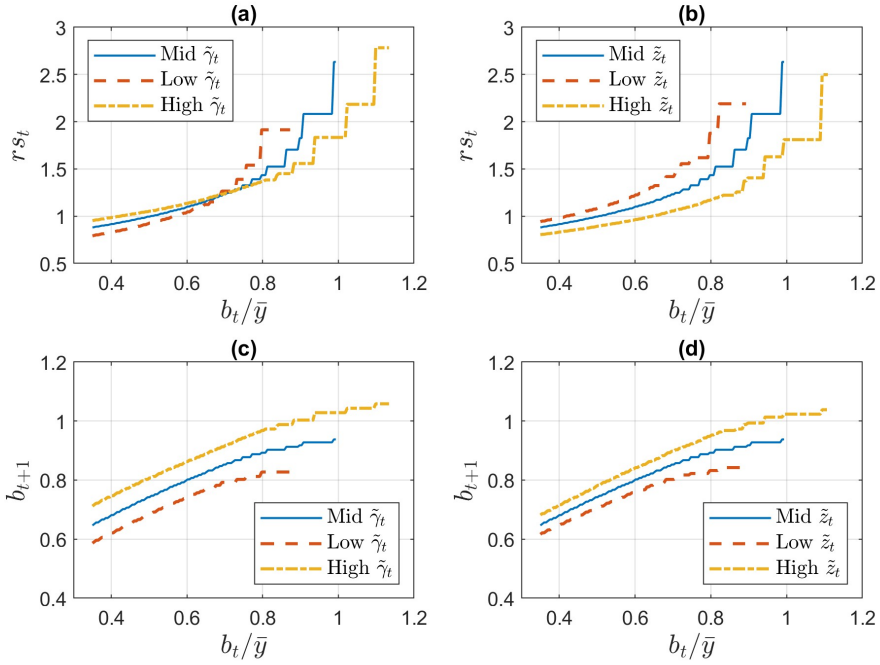

Figure 7: II model bond price schedules and issuance policies. "Mid $\tilde{\gamma}_t$" corresponds to the unconditional mean of trend beliefs; "High $\tilde{\gamma}_t$" and "Low $\tilde{\gamma}_t$" correspond to 2.3 standard deviations above and below the unconditional mean, respectively. $\tilde{z}_t$ levels in the right panels are defined analogously.

This amplification effect is particularly pronounced when spreads and outstanding debt $b_t/\bar{y}$ are already high – i.e., when rs_t is typically more sensitive to trend growth. As Table 7 shows, the II model generates $corr(rs_t, \tilde{\gamma}_t) = -0.42$ near spread peaks, compared with a much weaker -0.11 in the full sample. The FI model produces $corr(rs_t, \gamma_t) = -0.13$ around crises, but close to zero (0.02) in the full sample, consistent with Aguiar et al. (2016).

Asymmetric bond issuance policy responses contribute to this state dependence. Under mild financial stress featuring low debt-to-GDP ratios, negative trend shocks trigger rapid deleveraging and thereby reduce spreads. Figure 7 illustrates this mechanism using debt policy functions $\mathcal{B}(b_t, \mathbf{s}_t)$.

When outstanding debt is low ($b_t/\bar{y} < 0.7$), the optimal issuance policy ($b_{t+1} = \mathcal{B}(b_t, \mathbf{s}_t)$) under a low $\tilde{\gamma}_t$ lies below that under a higher $\tilde{\gamma}_t$ (panel (c)). This lower issuance translates

into lower spreads, as shown in panel (a). At higher debt levels ($b_t/\bar{y} > 0.7$), spreads become more sensitive to output shocks. Although bond issuance under low $\tilde{\gamma}_t$ remains lower than under a high $\tilde{\gamma}_t$, spreads in the low-trend case exceed those associated with higher $\tilde{\gamma}_t$.

In contrast, bond issuance responses to cyclical shocks are more symmetric. As shown in panel (d), when debt is low, comparable changes in cyclical shocks $\tilde{z}_t$ lead to smaller adjustments in bond issuance. Meanwhile, negative cyclical shocks raise spreads (panel (b)), unlike the spread-reducing effect of negative trend shocks shown in panel (a).

5.5 Overestimated trend during good time

The elasticity of bond issuance to trend shocks is especially relevant for understanding pre-crisis dynamics in GIIPS countries, when debt-to-GDP ratios were relatively low and GDP growth was strong. Figure 8 presents conditional impulse responses to (i) a positive shock to trend beliefs and (ii) a negative shock to the perceived cyclical component, with magnitudes and signs matching the evidence in Figure 1.[22] The responses are conditioned on debt-to-GDP ratios below 85% and on both the true and perceived output growth components being above their unconditional means, approximating conditions prior to 2009.

As panel (a) and (b) of Figure 8 illustrate, overestimating trend growth during good times initially improves perceived repayment capacity, reducing spreads mildly by about 30 basis points (bps) in the short term. However, this optimism about long-term growth also encourages rapid leveraging, reflected in the sharp rise in the B_t/Y_t ratio (panel (b)). The resulting increase in indebtedness subsequently pushes spreads to more than 60 bps above pre-shock levels. Such over-borrowing is widely cited as a key contributor to sovereign debt crises, e.g., Arellano and Bai (2017).

Panel (c) and (d) depict IRFs to a negative $\tilde{z}_t$ shock, representing an underestimation of the cycle. Spreads rise immediately by roughly the same amount as they fell in the trend-shock case. The debt-to-GDP ratio initially rises due to the contraction in Y_t, but as the sovereign cuts issuance, the ratio declines and spreads fall to about 15 bps below pre-shock levels. Compared with the positive $\tilde{\gamma}_t$ shock, the reduction in B_t/Y_t is smaller; therefore, pessimism about the cycle only partially offsets the long-term deterioration from trend optimism. Overall,

[22] In this experiment, agents believe a genuine trend or cyclical shock occurs at $t = 1$ (shocked paths), even though no such shock occurs in reality (unshocked paths). Agents treat the perceived shock as real and expect it to evolve according to the known process for γ_t or z_t.

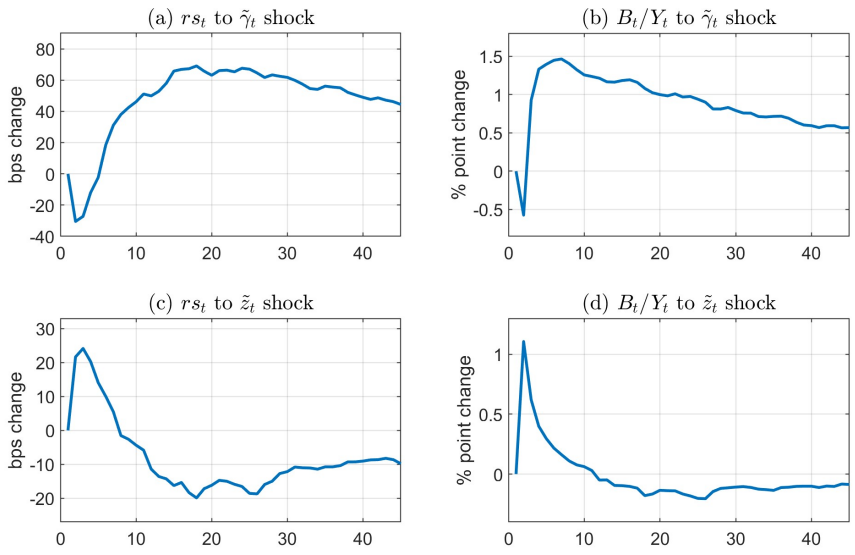

Figure 8: IRFs for the price schedule and bond issuance conditional on low debt-to-GDP ratios ($B_t/\bar{Y}_t \leq 0.85$) and output shocks above their unconditional means. Upper panels: response to a 0.6% shock to $\tilde{\gamma}$. Lower panels: response to a -1.6% shock to $\tilde{z}$.

the combination of trend optimism and cycle pessimism prior to 2009 likely increased both spreads and the debt-to-GDP ratio.

6 Conclusion

This paper studies how shifting long-run growth expectations influence sovereign debt pricing and borrowing dynamics during the 2010s Eurozone debt crisis. We document new empirical evidence of systematic errors in real-time estimates of long-run growth, as well as a negative and nonlinear relationship between these estimates and sovereign debt spreads.

We develop a sovereign default model in which agents learn about long-run output growth. Model simulations replicate key empirical patterns, including persistent errors in trend growth beliefs and a negative, nonlinear relationship between perceived trend growth and sovereign debt spreads. The model shows that optimism about long-run growth during booms encourages excessive borrowing, while pessimism during downturns amplifies debt distress. In contrast, a comparable full-information model generates substantially smaller fluctuations in debt spreads and fails to replicate these empirical regularities.

Our results highlight the critical role of perceived long-term output growth and belief dynamics in shaping sovereign debt spreads for Eurozone periphery countries around the Great

Financial Crisis. These findings suggest that reducing errors in official growth estimates—particularly excessive optimism during expansions—could improve debt sustainability and mitigate the severity of future crises. However, because estimating and forecasting long-run growth is inherently difficult, this remains a major challenge for policymakers and international institutions.

A large body of research has examined errors in economic growth forecasts. Evaluations of institutional forecasts (e.g., Timmermann, 2007; Chabin et al., 2020; Celasun et al., 2021) find that long-term projections from the WEO and EEF contain sizable errors. Internal reviews by the IMF and the European Commission have led to several recommendations aimed at mitigating "trend–cycle" confusion.

First, forecasters could communicate uncertainty more explicitly, for example by publishing risk distributions or fan charts (Turner, 2016; Chabin et al., 2020). Second, scenario analyses could explicitly incorporate large shocks—such as financial crises or trade disruptions—that may skew both macroeconomic outcomes (Ho and Mauro, 2016) and macro-financial risk assessments (Carrière-Swallow and Marzluf, 2022). Third, following downturns that reveal earlier overoptimism, forecasters should guard against systematic underprediction as an over-correction (Celasun et al., 2021). Finally, addressing behavioral features such as asymmetric responses to news and inertia in belief updating (Chabin et al., 2020) may improve the responsiveness and accuracy of growth forecasts.

Acknowledgements

This is a revised version of a chapter of Liang Shi's Ph.D. dissertation at the University of Birmingham. For valuable comments, we thank two anonymous referees, Kaushik Mitra, Yuemei Ji, Christoph Görtz, Anindya Banerjee, and seminar participants at the University of Birmingham, HUST China and University of Essex. All errors are our own.

Declaration

Conflict of interest: none.

References

Adam, K., Kuang, P., and Marcet, A. (2012). House price booms and the current account. *NBER Macroeconomics Annual*, 26(1):77–122.

Adam, K., Kuang, P., and Xie, S. (2025). Overconfidence in private information explains biases in professional forecasts. *Journal of Monetary Economics*, November.

Aguiar, M. and Amador, M. (2020). Self-fulfilling debt dilution: Maturity and multiplicity in debt models. *American Economic Review*, 110(9):2783–2818.

Aguiar, M., Chatterjee, S., Cole, H., and Stangebye, Z. (2016). Quantitative models of sovereign debt crises. *Handbook of Macroeconomics*, 2B:1697–1755.

Aguiar, M. and Gopinath, G. (2006). Defaultable debt, interest rates and the current account. *Journal of International Economics*, 69(1):64–83.

Aizenman, J., Hutchison, M., and Jinjarak, Y. (2013). What is the risk of european sovereign debt defaults? fiscal space, cds spreads and market pricing of risk. *Journal of International Money and Finance*, 34:37–59.

Arellano, C. and Bai, Y. (2017). Fiscal austerity during debt crises. *Economic Theory*, 64(4):657–673.

Arellano, C., Bai, Y., and Mihalache, G. (2018). Default risk, sectoral reallocation, and persistent recessions. *Journal of International Economics*, 112:182–199.

Auclert, A. and Rognlie, M. (2016). Unique equilibrium in the eaton–gersovitz model of sovereign debt. *Journal of Monetary Economics*, 84:134–146.

Ayres, J., Navarro, G., Nicolini, J. P., and Teles, P. (2025). Self-fulfilling debt crises with long stagnations. *Journal of Political Economy*, 133(12):4050–4101.

Baxter, M. and King, R. G. (1999). Measuring business cycles: approximate band-pass filters for economic time series. *Review of economics and statistics*, 81(4):575–593.

Blanchard, O. J. and Leigh, D. (2013). Growth forecast errors and fiscal multipliers. *American Economic Review*, 103(3):117–120.

Blanchard, O. J. and Leigh, D. (2014). Learning about fiscal multipliers from growth forecast errors. *IMF Economic Review*, 62(2):179–212.

Bocola, L. and Dovis, A. (2019). Self-fulfilling debt crises: A quantitative analysis. *American Economic Review*, 109(12):4343–4377.

Boz, E., Daude, C., and Durdu, C. B. (2011). Emerging market business cycles: Learning about the trend. *Journal of Monetary Economics*, 58(6-8):616–631.

Brock, W. A. and Hommes, C. H. (1997). A rational route to randomness. *Econometrica: Journal of the Econometric Society*, pages 1059–1095.

Carrière-Swallow, Y. and Marzluf, J. (2022). Macrofinancial causes of optimism in growth forecasts. *IMF Economic Review*, 71(2):509.

Celasun, O., Lee, J., Mrkaic, M., and Timmermann, A. (2021). An evaluation of world economic outlook growth forecasts—2004-17. *IMF Working Paper*, WP/21/216.

Chabin, A., Lamproye, S., and Vỳškrabka, M. (2020). Are we more accurate? revisiting the european commission's macroeconomic forecasts. *European Commission Discussion Paper*, 128.

Chatterjee, S. and Eyigungor, B. (2012). Maturity, indebtedness, and default risk. *American Economic Review*, 102(6):2674–99.

Christiano, L. J. and Fitzgerald, T. J. (2003). The band pass filter. *International Economic Review*, 44(2):435–465.

Coibion, O. and Gorodnichenko, Y. (2015). Information rigidity and the expectations formation process: A simple framework and new facts. *American Economic Review*, 105(8):2644–2678.

Coibion, O., Gorodnichenko, Y., and Ulate, M. (2018). The cyclical sensitivity in estimates of potential output. *Brookings Papers in Economic Activity*, pages 343–431.

Cole, H. L., Neuhann, D., and Ordonez, G. (2025). Information spillovers and sovereign debt: Theory meets the eurozone crisis. *Review of Economic Studies*, 92(1):197–237.

Cruces, J. J. and Trebesch, C. (2013). Sovereign defaults: The price of haircuts. *American economic Journal: macroeconomics*, 5(3):85–117.

De Grauwe, P. and Ji, Y. (2013). Self-fulfilling crises in the eurozone: an empirical test. *Journal of International Money and Finance*, 34:15–36.

De Grauwe, P. and Ji, Y. (2019). *Behavioural macroeconomics: Theory and policy*. Oxford University Press.

Durdu, C. B., Nunes, R., and Sapriza, H. (2013). News and sovereign default risk in small open economies. *Journal of International Economics*, 91(1):1–17.

Dvorkin, M., Sánchez, J. M., Sapriza, H., and Yurdagul, E. (2020). News, sovereign debt maturity, and default risk. *Journal of International Economics*, 126:103352.

Dvorkin, M., Sánchez, J. M., Sapriza, H., and Yurdagul, E. (2021). Sovereign debt restructurings. *American Economic Journal: Macroeconomics*, 13(2):26–77.

Eaton, J. and Gersovitz, M. (1981). Debt with potential repudiation: Theoretical and empirical analysis. *The Review of Economic Studies*, 48(2):289–309.

Edge, R. M., Laubach, T., and Williams, J. C. (2007). Learning and shifts in long-run productivity growth. *Journal of Monetary Economics*, 54(8):2421–2438.

Eusepi, S. and Preston, B. (2011). Expectations, learning, and business cycle fluctuations. *American Economic Review*, 101(6):2844–72.

Garcia-Cicco, J., Pancrazi, R., and Uribe, M. (2010). Real business cycles in emerging countries? *American Economic Review*, 100(5):2510–31.

Gordon, G. (2019). Efficient computation with taste shocks. Technical report, Federal Reserve Bank of Richmond.

Hamilton, J. D. (2018). Why you should never use the hodrick-prescott filter. *Review of Economics and Statistics*, 100(5):831–843.

Hatchondo, J. C. and Martinez, L. (2009). Long-duration bonds and sovereign defaults. *Journal of International Economics*, 79(1):117–125.

Hatchondo, J. C., Martinez, L., and Sosa-Padilla, C. (2016). Debt dilution and sovereign default risk. *Journal of Political Economy*, 124(5):1383–1422.

Havik, K., Mc Morrow, K., Orlandi, F., Planas, C., Raciborski, R., Röger, W., Rossi, A., Thum-Thysen, A., and Vandermeulen, V. (2014). The production function methodology for calculating potential growth rates & output gaps. *European Economy - Economic Papers 2008 - 2015*, 535.

Ho, G. and Mauro, P. (2016). Growth—now and forever? *IMF Economic Review*, 64(3):526–547.

Hodrick, R. J. and Prescott, E. C. (1997). Postwar us business cycles: an empirical investigation. *Journal of Money, credit, and Banking*, pages 1–16.

Irish Fiscal Advisory Council (2013). Fiscal assessment report. Technical report, Irish Fiscal Advisory Council, Dublin. April 2013.

Koop, G., Pesaran, M. H., and Potter, S. M. (1996). Impulse response analysis in nonlinear multivariate models. *Journal of Econometrics*, 74(1):119–147.

Kuang, P. (2014). A model of housing and credit cycles with imperfect market knowledge. *European Economic Review*, 70:419–437.

Kuang, P. and Mitra, K. (2016). Long-run growth uncertainty. *Journal of Monetary Economics*, 79:67–80.

Kuang, P. and Mitra, K. (2025). Potential output pessimism and austerity in the european union. *Journal of Money, Credit and Banking*, 57:1871–1905.

Kuang, P., Mitra, K., and Tang, L. (2024). Output gap estimation and monetary policy under imperfect knowledge. *University of Birmingham mimeo*.

Kuang, P., Mitra, K., Tang, L., and Xie, S. (2026). Macroprudential policy and housing market expectations. *European Economic Review*, 181.

Lorenzoni, G. and Werning, I. (2019). Slow moving debt crises. *American Economic Review*, 109(9):3229–3263.

Mihalache, G. (2020). Sovereign default resolution through maturity extension. *Journal of International Economics*, 125:103326.

Na, S., Schmitt-Grohé, S., Uribe, M., and Yue, V. (2018). The twin ds: Optimal default and devaluation. *American Economic Review*, 108(7):1773–1819.

Niemann, S. and Prein, T. M. (2025). Sovereign risk under diagnostic expectations. Working Paper 2025-02, Department of Economics, University of Konstanz.

Paluszynski, R. (2023). Learning about debt crises. *American Economic Journal: Macroeconomics*, 15(1):106–134.

Schmitt-Grohé, S. and Uribe, M. (2012). What's news in business cycles. *Econometrica*, 80(6):2733–2764.

Stangebye, Z. R. (2020). Beliefs and long-maturity sovereign debt. *Journal of International Economics*, 127:103381.

Timmermann, A. (2007). An evaluation of the world economic outlook forecasts. *IMF Staff Papers*, 54(1):1–33.

Tomz, M. and Wright, M. L. (2007). Do countries default in "bad times"? *Journal of the European Economic Association*, 5(2-3):352–360.

Turner, D. (2016). The use of models in producing oecd macroeconomic forecasts. *OECD Economics Department Working Papers*, No. 1336.

Uribe, M. and Schmitt-Grohé, S. (2017). *Open Economy Macroeconomics*. Princeton University Press.

Yue, V. Z. (2010). Sovereign default and debt renegotiation. *Journal of International Economics*, 80(2):176–187.